FINAL REPORT

ADSORPTION OF HYDROGEN CHLORIDE ON MICROCRYSTALLINE SILICA

by

Yoonok Kang and James P. Wightman

Prepared for

National Aeronautics and Space Administration

January, 1979

Grant NSG-1389

NASA-Langley Research Center
Hampton, Virginia 23665
Space Applications and Technology Division
Dr. Gerald L. Pellett

Department of Chemistry
Virginia Polytechnic Institute and State University
Blacksburg, Virginia 24061

TABLE OF CONTENTS

Page

LIST OF TABLES

LIST OF FIGURES

I. INTRODUCTION

Hydrogen chloride gas is a well known toxic compound. A trace of hydrogen chloride is found naturally as a result of volcanic activity. However, increasing concentration of this gas in the environment produced as a by-product of some manufacturing processes[1-3] is of great concern. This concern is reflected in the various studies of the impact of hydrogen chloride on the environment. Such studies as the damage of hydrogen chloride to plants and animals,[4,5] air pollution from the combustion of poly(vinyl chloride),[6] and 'atmospheric reduction' of chlorinated compounds into hydrogen chloride[7] are some of the many examples.

Another source of HCl is the combustion of the solid propellant to be used in the space shuttle. The first Space Shuttle is scheduled to be launched in late 1979. Hydrogen chloride is produced during combustion and constitutes 21% of the exhaust products[8] as shown in Table I. A total of 212000 kg (233 tons) of HCl are produced in a typical launch and about 20 tons of HCl are assumed to be in the ground cloud. The interaction of this hydrogen chloride with the environment and other exhaust products may be quite complicated. The National Aeronautics and Space Administration (NASA) has an extensive program designed to assess the impact of hydrogen chloride and other exhaust products on the environment. An appreciable amount of ground debris is swept upward by the force exerted by the rocket exhaust gases upon launching. Analysis of soil adjacent to the launch pad indicates about 88% quartz composition.[9] Thus the interaction of

Table I. Mass fractions of the various chemical species constituting the exhaust gas mixture at the nozzle exit plane of a Solid Rocket Motor (SRM)

Exhaust Component	Mass Fraction
Al_2O_3 (l and s)*	0.30
CO	0.23
HCl	0.21
H_2O	0.10
Others	Balance

*Unless otherwise noted by l (liquid) or s (solid), the species are in the gaseous phase.

hydrogen chloride with quartz, crystalline silica, is expected and is of interest. For example, to what extent does the ground debris remove hydrogen chloride produced in the exhaust from the atmosphere?

The objective of this work was to characterize the interaction of hydrogen chloride with silica, silicon dioxide, and specifically, the extent to which silica can irreversibly remove hydrogen chloride from the atmosphere. Adsorption isotherms were measured at 30°C for hydrogen chloride on silica outgassed between 100° and 400°C. Readsorption isotherms were also measured. The silica surface was characterized further by infrared spectroscopy, electron spectroscopy for chemical analysis (ESCA), scanning electron microscopy (SEM), and immersional calorimetry. This study also included similar work on ground debris samples obtained from the Kennedy Space Center.

II. LITERATURE SURVEY

This section covers the literature survey related to the adsorption of hydrogen chloride on silica. The survey will be limited to the quartz system in most cases since there are so many different types of silica. General references on adsorption include Gregg and Sing,[10] Flood,[11] and Schulman.[12]

A. Solid Rocket Propellant Exhaust

The National Aeronautics and Space Administration has been involved extensively with environmental impact studies on the solid rocket exhaust. There is speculation that the exhaust products which pass through the high temperature shock wave reform and might have different effects on the environment than that of the original products.[13] An extensive literature survey on the solid propellant exhaust products and related studies was done by Bailey.[14] Bailey studied the interaction of two of the major exhaust products, hydrogen chloride and alumina. By studying the adsorption isotherms, it was found that although water vapor adsorption is physical and a reversible process, hydrogen chloride adsorption is in part chemical and about 60% irreversible. Cofer and Pellet[15] have studied adsorption of hydrogen chloride on alumina in a flow system employing the gravimetric adsorption technique. Partial pressure of hydrogen chloride and water were adjusted in nitrogen carrier gas. It was found that about 50% of the total adsorption was the chemisorbed weight gain and about one half of the chemisorbed weight gain was due to chloride ions.

B. Silica and Its Surface

General references on silica are provided by several authors.[16-18] Sosman authored one volume on twenty-two phases on silica[18] and a classic monograph is available on the physical properties of silica.[17] Also, 4000 phase diagrams on silica have been compiled by the American Ceramic Society.[19]

Silica is found in nature as the crystalline varieties, non-crystalline or amorphous, crysto crystalline, and as vitreous silica.[20] The crystalline varieties are further classified as quartz, tridymite and crystobalite based on their thermal stability. Each of the crystalline varieties has α and β phases existing at low and high temperatures, respectively, and phase transitions involve changes of symmetry and density. The temperature dependence of the transition of the crystalline silicas is as follows:

$$\text{Quartz} \overset{870^{\circ}C}{\rightleftharpoons} \text{Tridymite} \overset{1470^{\circ}C}{\rightleftharpoons} \text{Crystobalite} \overset{1700^{\circ}C}{\rightleftharpoons} \text{Vitreous}^{21}$$

The different varieties of crystalline and amorphous silica have very similar chemical properties except for the reactivity. General trends of reactivity are as follows:

$$\text{Quartz} < \text{Tridymite} < \text{Crystobalite} < \text{Amorphous}^{22}$$

The structure of the unit cell of both α and β phases of quartz is suggested to be hexagonal and composed of three atom triplets of silica which satisfies the octet rule configuration[23] as shown in Figure 1.

It is generally accepted that the surface of silica is hydroxylated with different types of hydroxyl groups.[24-26] Davydov, et al.,

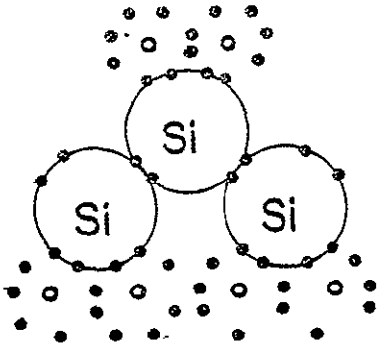

Figure 1. Electronic Structure of the Silica Molecule

reported[27] that there are three kinds of surface hydroxyl groups on the silica surface namely, the free hydroxyl, hydrogen bonded hydroxyl, and internal hydroxyl which give infrared absorption bands at 3750 cm^{-1}, 3650 cm^{-1}, and 3550 cm^{-1}, respectively. Hambelton and Hockey[28] have given a good pictorial representation of the three types as shown in Figure 2.

Davydov[29] indicated that upon evacuation at 400°C, only 50% of the original hydroxyl groups remain and are all free hydroxyl groups. However, the number of free hydroxyl groups is decreased when evacuated above 400°C.[30] Hair[31] suggested a dehydroxylation mechanism as follows:

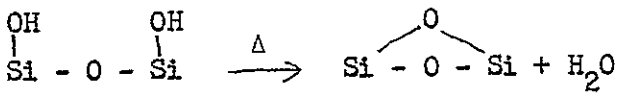

The changes in the nature of hydroxyl groups on the silica surface upon evacuation at various temperatures were intensively studied by Boccuzzi, et al.[32]

It has been shown that free hydroxyl groups play the major role in specific adsorption.[33,34] The concentration of hydroxyl groups on the silica surface has been studied by many authors using different techniques including gravimetric methods,[35,36] chemical reactions,[37,38] deuterium exchange,[27] and most frequently by infrared spectroscopy.[24,25] To overcome the difficulty of characterizing quartz of low surface area, free radical spin labels were employed.[39] Based on a calculation assuming one hydroxyl group per silicon atom, quartz with density of 2.655 has a maximum of 9 hydroxyl groups per 100 $Å^2$ on its surface.[40] However, it is generally assumed that the average number of hydroxyl

a. Free hydroxyl

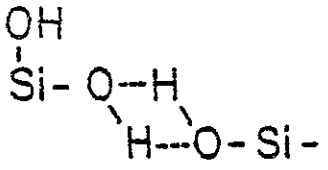

b. H-bonded hydroxyl

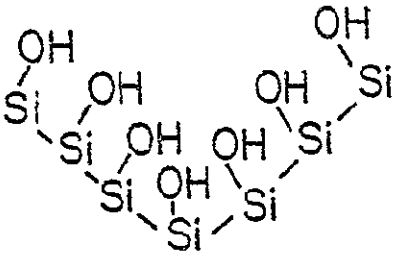

c. Internal hydroxyl

Figure 2. Three Types of Hydroxyl Groups on the Silica Surface.

groups on the crystalline silica surface is 4 or 5 per 100 $Å^2$.[41] However, the number of hydroxyl groups varies considerably with the evacuation parameters such as time, temperature, and pressure.

C. HCl as an Adsorbate

Hydrogen chloride has not been a commonly used adsorbate. Studies on the adsorption of hydrogen chloride on ZnO, $AlPO_4$, and on TiO_2 were reported at the Faraday Discussion in 1971.[42] In all cases, the adsorption of hydrogen chloride was found to be minimal and partially irreversible. OH concentration on TiO_2 surface was reported to be influenced by chemisorption of hydrogen chloride on TiO_2.[43] Bailey[14] and Pellet[15] studied the adsorption of hydrogen chloride gas on alumina, whereas Tyree[44] worked with Al_2O_3 - HCl_{aq} system.

Although there have been numerous studies done on the adsorption of various gases on silica, not much work has been done with hydrogen chloride. Kiselev reported weak adsorption of hydrogen chloride on silica.[45] Peri studied hydrogen chloride gas on the dry aerosil plates with IR and concluded that hydrogen chloride does not chemisorb on aerosil.[46] The study of hydrogen chloride adsorption on quartz has not been reported.

D. Surface Techniques

There is a recent review on the techniques used in surface analysis.[47] Although infrared spectroscopy is the most frequently used technique because of its simplicity, ESCA, Auger-electron spectroscopy (AES), and secondary-ion mass spectroscopy (SIMS) are some of many developing powerful surface analytical techniques. ESCA

is used widely since its introduction by Siegbahn, et al.[48] In fact, a recent Faraday Discussion was devoted entirely to ESCA.[49] Hercules has reported extensive work on the theory, instrumentation, and application of ESCA.[50] Powell[51] discussed quantitative analysis by ESCA using a simple three step model for electron generation, transport to the surface, and detection. Angular studies done with ESCA[52] have proved useful in the further characterization of surface layers. Nefedov and Salyn[53] have compared the binding energies of many compounds including silica measured by different types of ESCA and showed the consistency in them.

Calorimetry is another technique frequently used in surface chemistry for the measurement of heats of wetting or heats of immersion. Whalen reported the heats of immersion ($\Delta_W H$) of various types of silica including quartz in water.[35] Heats of immersion for quartz were different depending on the size of the particles. The larger particles showed higher heats of immersion. Samples with a greater number of surface hydroxyl groups had lower heats of immersion.

Tschapek, Bussetti and Ardizzi studied the interaction of $HCl_{(aq)}$ and $HNO_{3(aq)}$ with aerosil.[54] It was found that at pH <3, the following reaction occured;

$$SiOH + HCl \longrightarrow SiOH_2^+ + Cl^-$$

Heats of immersion increased with increasing acid concentration. Samples outgassed at 800°C yielded a value only one half of heats of immersion of ones outgassed at 110°C. This is consistent with the previous report by Young[30] that almost all OH groups are removed by

evacuation at or above 800°C so that the adsorption of acid might be 1 molecule per 2 atoms of Si as follows:

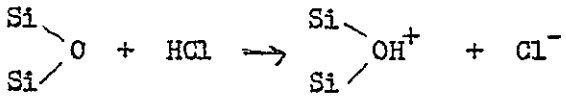

No heats of immersion of quartz in $HCl_{(aq)}$ have been reported.

III. EXPERIMENTAL

This section contains a description of the materials used, experimental procedures for various techniques, and the calculations for the data reduction employed in this study.

A. Materials

1. Adsorbates: Nitrogen and hydrogen chloride were used as adsorbates. Dry nitrogen from the Airco Company was used in the surface area measurement and anhydrous hydrogen chloride from the Matheson Company was used for the adsorption isotherm study.

2. Adsorbents: The microcrystalline silica, used in the study, was Min-U-Sil 5 produced by a proprietary process and supplied by the Pennsylvania Glass Sand Corp. According to the manufacturer, the average particle size is $<5\mu$. An x-ray diffraction pattern indicated that Min-U-Sil 5 was quartz.

NASA ground samples were also used as adsorbents. NASA provided the ground samples collected from two different locations at the Kennedy Space Center. Samples #2 and #4 were collected at locations 2300 ft, 73° and 9600 ft, 180° from the launch complex 40, respectively after a launch. The samples were collected with a vacuum sweeper and were given no other treatment. Samples labelled "pre-launch" and "post-launch" were collected directly from the launch pad.

3. Miscellaneous: 49.3% HF solution obtained from the Baker Chemical and NaOH pellets from the Fisher Scientific were used for the removal of amorphous layers on the silica surface. Hellige standard

hydrochloric acid solution (R1193c) was diluted to 1ℓ with deionized water to prepare 0.1N HCl stock solution for the calorimetric studies. Helium used for the calibration of volumes in the adsorption study was obtained from the Airco Company.

B. Surface Area Measurement

Surface areas, based on the BET theory described by Gregg and Sing,[10] were measured using the Micromeritics Model 2100D Orr Surface Area and Pore Volume Analyzer. The 2g silica samples were outgassed at 100°C and 400°C for 2 hours at about 1×10^{-5} torr and the 4g NASA samples were outgassed at 100°C for 15 minutes prior to the surface area measurement. To check the effect of the outgassing period on the surface area, one silica sample was outgassed at 100°C for 15 minutes. Calibration of the volume of the pyrex sample bulbs was done with helium and nitrogen was used as the adsorbate for the measurement. The cross sectional area of an adsorbed nitrogen molecule was taken as 16.2 Å^2. The computer program in Appendix I was written by Skiles[55] and used to calculate the surface areas.

C. Adsorption Isotherms

Adsorption isotherms were measured to study the uptake of hydrogen chloride by silica outgassed at different temperatures. The apparatus and procedure are described below.

1. Apparatus: The schematic diagram of the Pyrex vacuum system is given in Figure 3. The system can be divided into three basic sections: vacuum system (A), auxiliary section (B), and critical section (C).

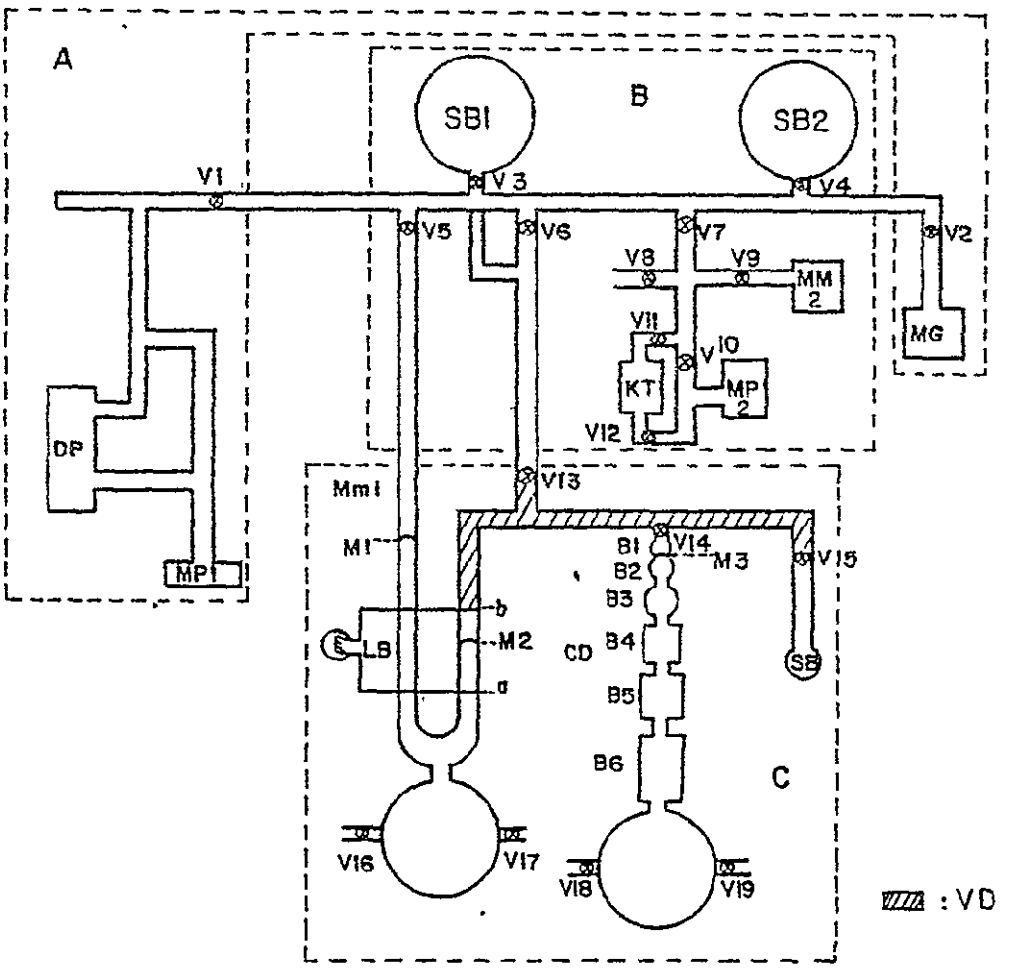

Figure 3. Vacuum Line for the Adsorption Study.

The vacuum system was consisted of a mercury diffusion pump (DP) and a mechanical pump (MP1). Typical base pressures obtained were between 1×10^{-5} and 1×10^{-6} Torr. The pressure was read with a McLeod gauge (MG).

The auxiliary section included the introduction, storage, and removal of the reactant gases from the system. Gases were introduced through valve V8 and stored in the storage bulbs SB1, and SB2. The pressure of the gas put into the system was measured by the manometer (MM2). HCl was removed through KOH pellet trap (KT) by the mechanical pump (MP2).

The adsorption measurements were made at the critical section. It consisted of a manometer (MM1), precalibrated doser (CD) with 6 bulbs (B1 - B6), light bulb (LB), and the sample bulb (SB). The sample bulb was either immersed in a constant temperature water bath or surrounded by a furnace. The water bath temperature was maintained constant by a mercury thermoregulator connected to a Fisher Model 51 Unitized Bath Control. A Hoskins Electric Furnace was used and its temperature controlled by a powerstat.

2. Calibration of the doser: The weight of mercury in each of the six bulbs of the doser (CD) was measured. The volume of each bulb was determined from the measured weight and the known density of mercury at ambient temperature.

3. Evacuation: System valves except for V3-V5, V7, V8, V15-V19 were opened. The pressure was taken with the McLeod Gauge (MG).

4. Introduction and removal of gases: Valves V1 -V5, V10, V11, V13, V16-V19 were closed and gas was introduced through V8. The system was flushed 3 times. Pressure was measured with the manometer (MM2), and typically about 760 torr was introduced at one time. Then the gas was stored in one of the storage bulbs (He in SB2 and HCl in SB1). Excess helium was removed directly through the diffusion pump (DP) by opening V1. HCl was removed through the KOH trap (KT) through V11 and V12 slowly (~1 mm Hg per second).

5. Achievement of constant volume: A constant volume was achieved with the aid of the light (LB). One end of the circuit wire was immersed in mercury (a), and the other end was placed at a fixed position (b). By controlling the meniscus of the mercury (M2) with either V16 and/or V17 to barely touch the wire tip at b, the light blinked. This ensured the achievement of a constant volume.

6. Calibration of the dead volume: The system was first evacuated as described above. The height of the mercury meniscus (M2) was adjusted so that the light (LB) would blink. The location of the other arm of the meniscus (M1) was read with the cathetometer (Gaertner Scientific, precision $\pm$ 0.05 mm). This 3 step procedure will be refered as "taking a reference pressure reading" from here on. With only valves V6, V13, and V14 opened, helium was introduced into the system from the storage bulb. The pressure reading was taken by adjusting the reference arm of the meniscus (M2) to position b and taking the location of the M1 with the cathetometer. From

here on, this process will be referred to as "taking the pressure reading." The meniscus of the mercury inside the doser (M3) was then moved down with valve V18 and/or V19 to each bulb level and the corresponding pressure was taken. With this series of pressure measurements and with the known volumes of the bulbs, the value of the dead volume (VD) was calculated.

7. Adsorption measurement: In a sample bulb (SB), 2 g of adsorbent was placed and the sample was outgassed at 100°C, 200°C, and 400°C for 2 hours prior to the adsorption measurement. The isotherms were taken at 30°C maintained by the water bath. The volume of the sample bulb was determined with helium with valve V15 closed. Helium was introduced into the system as mentioned above. Valve V13 was closed and the pressure reading was taken, typically about 200 Torr. Valve V15 was then opened and helium was allowed to expand into the sample bulb (SB). The pressure reading was taken again and then helium was removed. The vacuum was checked again and the reference pressure reading was taken. Valves V6 and V15 were closed and HCl was introduced into the system through V3. (Approximately 7 Torr for each dose.) V13 was closed and a pressure reading (P_{ini}) was taken. V15 was then opened to start the adsorption. The system was allowed to equilibriate for an hour to reach the steady state and then the equilibrium pressure was taken (P). Application of HCl was repeated until the isotherm was completed. From the second dose on, the equilibrium pressure reading was taken half an hour after the introduction of HCl. HCl was removed from the system as described above.

8. Readsorption isotherm: The readsorption isotherm was taken to study the reversibility of the adsorption process. After the completion of the adsorption isotherm, the sample bulb was evacuated at 30°C for overnight (about 20 hours) or at 100°C and 400°C for 2 hours. Then the adsorption isotherm was taken as before.

D. Electron Spectroscopy for Chemical Analysis (ESCA)

A DuPont 650 electron spectrometer with Mg K_α radiation (1254 eV) was used in the study to characterize the surface of the sample. Normal operating pressure for the analyzer was about 1×10^{-7} Torr.

ESCA spectra were taken for fresh samples and samples after the hydrogen chloride adsorption/readsorption study. Samples were removed from the vacuum system and exposed to atmosphere before the ESCA analysis. Samples were hand pressed onto the brass probe when possible. When the hand-pressing technique failed, Scotch double stick adhesive tape was used to place the sample on the probe. The probe was cleaned with either methanol or acetone before sample mounting. For the angular studies, probes with take-off angles of 30°, 11°, and 6° were used. An additional ESCA analysis was done by varying the temperature of the sample probe from ambient (~40°) to 400°C.

Wide scan ESCA spectra of pure silica and NASA samples were taken. For the narrow scans, the spectra of the Si 2s, C 1s, O 1s, and Cl 2p photopeaks were taken. Binding energies of elements were corrected taking the binding energy of the C 1s photopeak as 284.0 eV.

E. Calorimetry

Heats of immersion were determined in a Calvet Microcalorimeter (MS-70). A schematic diagram of the sample cell and the sample chamber is given in Figure 4. Calibration of the system was done by passing a measured current (I) for a known period of time (t) through a resistor (R = 1001.0) in the sample cell. The output signal from the calorimeter was amplified and integrated to give a characteristic number of counts (C). The sensitivity of the calorimeter (S) was determined using the equation

$$S = \frac{I^2Rt}{C} \quad \text{(Joules/count)} \qquad (1)$$

Four sample chambers were matched as two pairs (cells 1 and 2, cells 3 and 4) and one cell was used as a reference while heats of immersion were measured for the other.

Sample bulbs containing 0.5 g of silica were outgassed at 100°, 200°, and 400°C for 2 hours and sealed under vacuum. Sealed sample bulbs were attached to a breaker rod and were put in a sample cell containing 2 ml of 0.1, 0.01, and 0.001 N HCl (aq). This assembly was then placed in the calorimeter and allowed to reach the steady state. Typically, it took about an hour to reach the steady state which was arbitrarily defined as three consecutive 100 seconds printouts of a constant number. When the initial steady state is reached, the rod was pressed to break the fragile tip of the sample bulb to initiate the reaction. A typical sensitivity setting of the

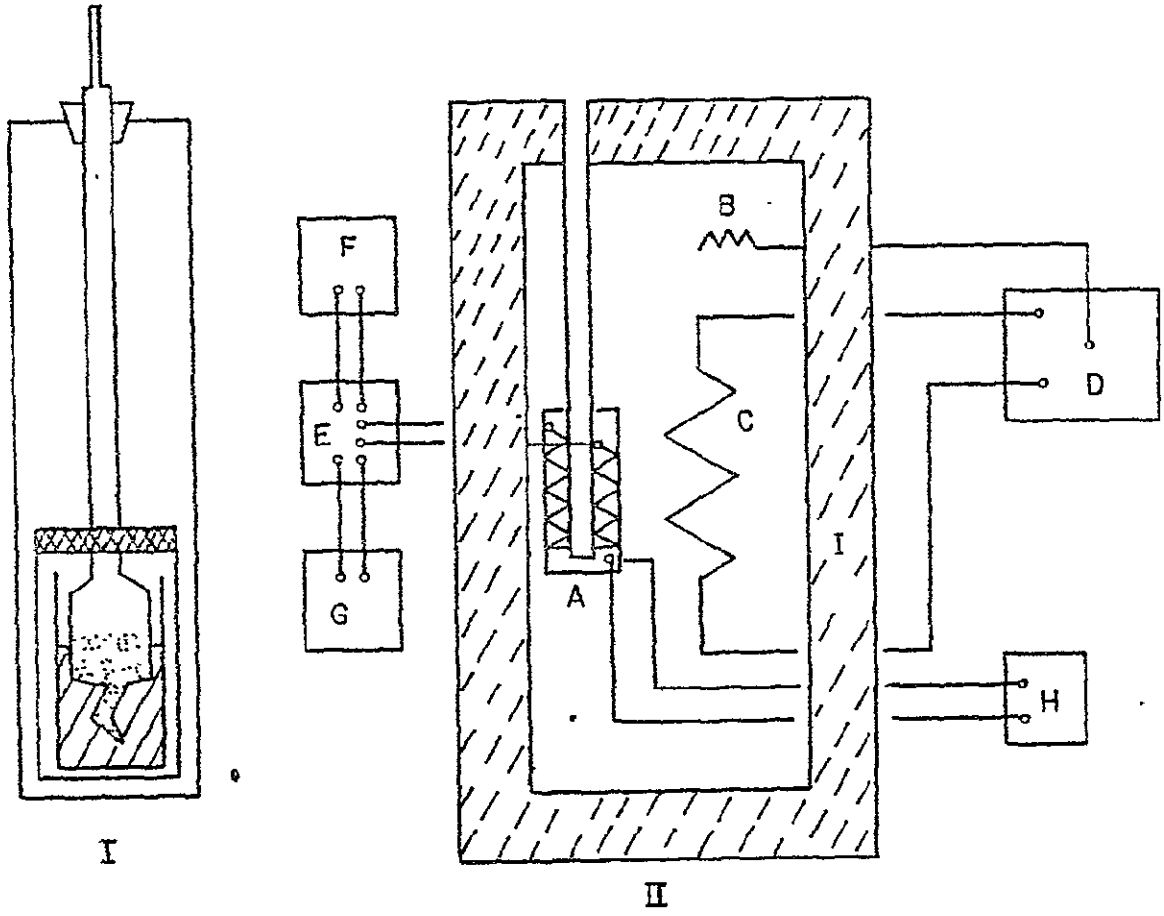

Figure 4. Schematic Diagram of Calorimeter Sample Cell (I) and Chamber (II)

A: Microcalorimetric element (detector
B: Temperature regulator probe
C: Temperature regulator heater
D: Temperature regulator
E: Amplifier
F: Recorder
G: Integrator counter
H: Platinum resistance thermometer
I: Insulation

calorimeter was GS x 100 or GS x 250 with a sensitivity of about 2×10^{-4} and 5×10^{-4} Joule per count, respectively.

F. Scanning Electron Microscopy (SEM)/Energy Dispersive Analysis of X-rays (EDAX)

The characteristic appearance of the particles was studied with an Advanced Metal Research Corporation Model 900 scanning electron microscope. The microscope operates at 20 kV and has an International Model 707A energy dispersive analysis of x-rays (EDAX) accessory. Silica after different treatments and the NASA samples were examined at various magnifications. Copper conductive tape was used to place the sample on the probe. A thin film of Au/Pd alloy was vacuum coated on the sample to decrease the charging on the sample. EDAX was employed for the x-ray analysis of elements with atomic number ≥ 11.

G. Infrared Spectroscopy

Infrared spectra were taken with a Perkin Elmer Model 283 spectrophotometer. The spectrum of silica before and after equilibration with HCl was taken under ambient conditions. The sample was rubbed on a NaCl crystal and another crystal of NaCl was used as a reference. Ordinate expansion (x10) was used in the 4000-3000 cm^{-1} region.

H. Removal of the Amorphous Layer

It is generally accepted that the surface of quartz is covered with an amorphous layer.[56-58] Therefore, it was of interest to study the interaction of HCl with a quartz surface free of an amorphous layers. The amorphous layer was removed by HF.[58,59] 20 g of silica

was placed in 100 ml of 10% HF (diluted from 49.5% HF with deionized water) for 5 minutes. It was then washed with 200 ml of 0.1N NaOH solution and 200 ml of deionized water. The treated silica which will be referred to as 'Iler treated silica', was dried at about 115°C for 1 hour.

Adsorption isotherms of HCl were taken at 30°C for the Iler treated silica out-gassed at 100°C for 2 hours. ESCA, calorimetry and SEM/EDAX analyses were also done on the Iler treated sample.

I. Data Reduction

1. Surface area: Surface areas were calculated using the computer program listed in Appendix I.

2. Adsorption isotherm: The ideal gas equation was used assuming constant temperature.

The dead volume (VD) was calculated by the following relations:

$$P_{VD} \times VD = P_{Bi} \left(VD + \sum_{i=1}^{i} V_{Bi}\right) \tag{2}$$

$$VD = \frac{P_{Bi} \times \sum_{i=1}^{i} V_{Bi}}{P_{VD} - P_{Bi}} \tag{3}$$

where, P_{VD} is the pressure of helium inside the dead volume (VD), V_{Bi} is the volume of individual bulbs, and P_{Bi} is the pressure inside the volume of $VD + \sum_{i=1}^{i} V_{Bi}$.

The number of HCl molecules was calculated from known pressure, volume and temperature. The difference between the initial (before exposure to sample) and final (after equilibration with the sample) number of molecules present in the gas phase was considered as being 'adsorbed' on the solid surface. The relevant equations are as follows:

$$N_{ini} = \frac{P_{ini} \times VD}{RTW \cdot a_s} \tag{4}$$

$$N_{fin} = \frac{P \times (VD + V_{SB})}{RTW \cdot a_s} \tag{5}$$

$$N_i^s = N_{ini} - N_{fin} + \frac{P_{i-1} \times V_{SB}}{RTW \cdot a_s} + N_{i-1}^s \tag{6}$$

where, P_{ini} is the pressure in the dead volume (VD) prior to each exposure of HCl to sample and P is the equilibrium pressure in the system after the HCl exposure. V_{SB} is the volume of the sample bulb. W is the weight of the sample and a_s is the specific surface area. N_{ini} and N_{fin} are the number of gas phase molecules in the system before and after the exposure of HCl, respectively. R is the gas constant.

3. Calorimetry: Heats of immersion ($\Delta_w H$) were calculated using the equation,

$$H = \frac{S \times C - B}{W \times a_s} \tag{7}$$

where S is the calorimeter sensitivity, C is the measured number of counts, B is the heat evolved from the empty bulb breaking, W is the sample weight, and a_s is the specific surface area.

4. ESCA: Intensities were corrected with published respective photoionization cross sections.[60] The photoionization cross sections ( ) used for Si 2s, O 1s, C 1s and Cl 2p are 0.855, 2.85, 1.00, and 1.564, respectively. Atomic fractions were obtained from,

$$\frac{I_i/}{\sum_{i=1}^{n} I_i/} \qquad (8)$$

where I_i is the intensity of each significant peak in the ESCA spectrum of the sample.

IV. RESULTS AND DISCUSSION

Part I: SILICA

A. Characterization

1. X-ray diffraction: The result of an x-ray diffraction pattern indicated that Min-U-Sil 5 is α-quartz. The x-ray spacings for untreated silica were 4.24 and 3.34 Å and for Iler treated silica were 3.35 and 4.25 Å. These spacings agree with published x-ray diffraction patterns for α-quartz.[61] The 3.34 Å spacing for Min-U-Sil 5 was also observed by Edmonds.[62]

2. Surface area measurements: Surface areas of silica outgassed at 100°C and at 400°C for 2 hours are tabulated in Table II. The symbol 'OGT' means outgas temperature. 'Old' and 'new' silica batches were dated June 1971 and March 1972, respectively. Although the calculation of the surface areas was done by computer, a typical BET plot for silica outgassed at 100°C for 15 minutes is shown in Figure 5. Similar plots were obtained for other samples.

There was no significant difference in the measured surface area of the two batches of silica. There seemed to be a small increase in surface area with higher outgassing temperature. However, it is generally accepted that the surface area of amorphous silica shouldn't vary in the temperature range 100°C to 400°C. Thus, all subsequent calculations were done using 5.06 m^2/g as the average value of the surface area of silica.

Table II. Surface areas of silica outgassed at various temperatures.

	Untreated Silica		Iler Treated Silica	
	OGT 100°C	OGT 400°C	OGT 100°C	OGT 400°C
Old	5.07 m^2/g 5.09	5.23 m^2/g 5.24	3.06 m^2/g 2.83 2.63	3.21 m^2/g 3.35 3.38 3.39
New	5.04 5.05	5.54 5.29		
Ave.	5.06±0.02	5.33±0.15	2.84±0.22	3.33±0.08

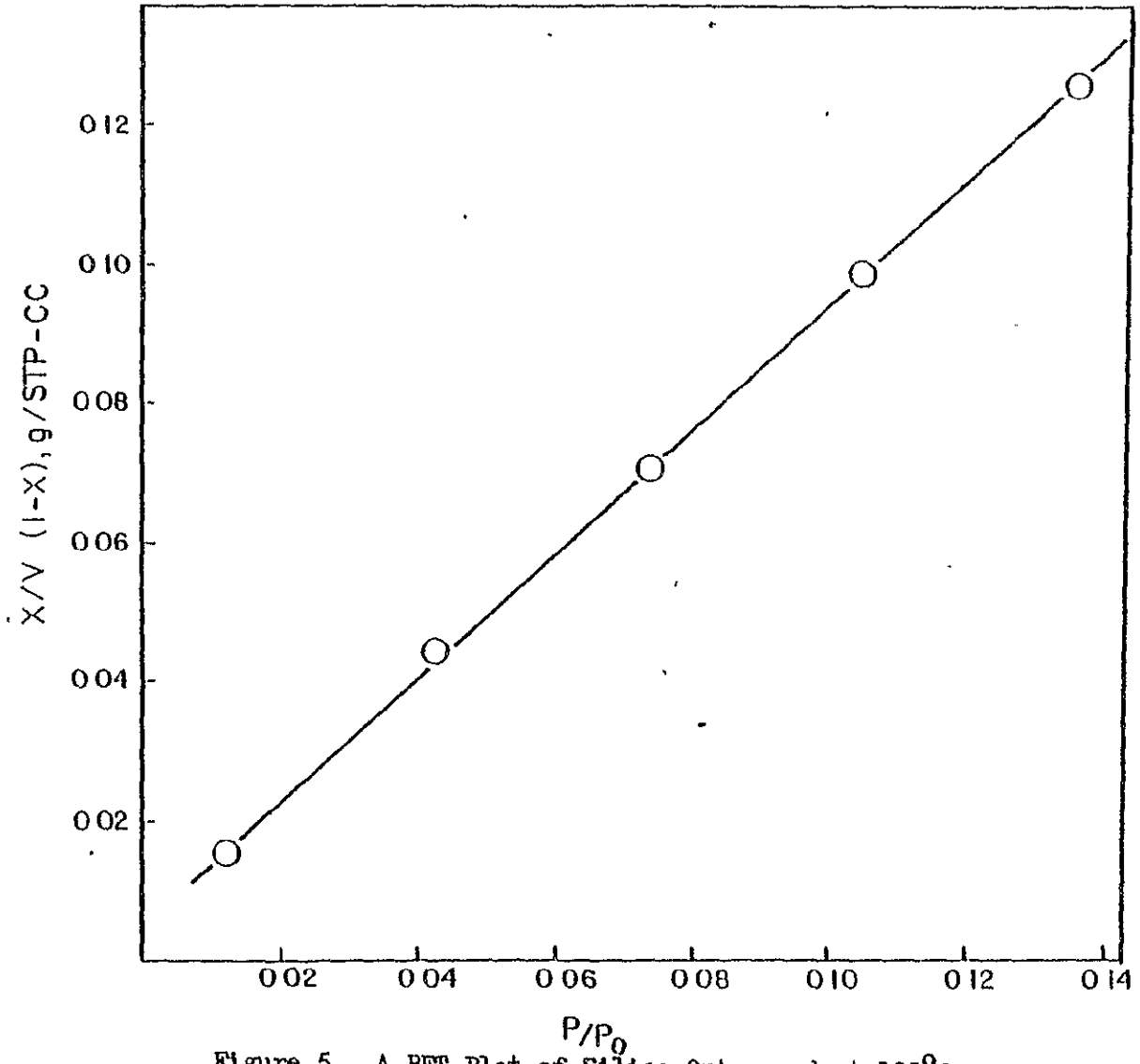

Figure 5. A BET Plot of Silica Outgassed at 100°C.

The surface area of the Iler treated silica was significantly lower than that of untreated silica. For Iler treated silica, the average surface area was taken as 2.84 m^2/g. This observed decrease in surface area supports the general recognition that an amorphous surface layer is present on quartz.[56-58] If the untreated surface was also crystalline, a higher specific surface area would be expected after etching due to a decrease in particle size. Again, a small increase in surface area with higher outgassing temperature was observed.

There was no significant difference in the surface area between samples outgassed at 100°C for either 15 minutes or for 2 hours. The measured surface area of silica outgassed at 100°C for 15 minutes was 4.94 m^2/g.

3. ESCA:

a. Hydrocarbon contamination: Hydrocarbon contamination is often seen in ESCA studies resulting from exposure to organic compounds prior to and during analysis. In any case, the contamination level as monitored by the intensity of the C 1s photopeak was found to increase with respect to time during the ESCA analysis of silica. Table III shows the result of four series of ESCA spectra of C, Si, and O taken sequentially on silica. The time span for each series was about 10 min. Notice that the atomic fraction ratio of O to Si is greater than 2. This was an unexpected result. Nonetheless, the value of the O to Si ratio remained constant whereas the value of the C to Si ratio increased significantly. This indicated that hydrocarbon contamination is occuring during the ESCA analysis but such contamination does not alter the O to Si ratio.

Table III. Binding energies (B.E.) and atomic fractions (A.F.) of C, Si, and O in silica taken in series

	C		Si		O			
Series	B.E.(eV)	A.F.	B.E.(eV)	A.F.	B.E.(eV)	A.F.	O/Si	C/Si
1	284.0	0.166	153.4	0.221	531.7	0.606	2.7	0.75
2	284.0	0.206	153.4	0.213	531.7	0.576	2.7	0.97
3	284.0	0.240	153.5	0.208	531.8	0.548	2.6	1.15
4	284.0	0.272	153.2	0.200	531.6	0.524	2.6	1.36

The effect of temperature on the hydrocarbon level was investigated also. ESCA spectra were taken on untreated silica at ambient probe temperatures of 40°, 100°, 200°, 300°, and 400°C. The results are tabulated in Table IV. Again relatively constant O/Si ratio was observed and was >2. The value of the C/Si ratio increased up to 200°C and then decreased significantly. Thus appreciable amounts of carbon was removed at high probe temperature.

The observed consistency in O/Si ratio for both studies indicated that the hydrocarbon contamination was not from oxy-carbon compounds. The results also implied that oxygen from adsorbed water was not responsible for the observed higher values of the O/Si ratio.

b. Silica: The wide scan (taken from 700 eV) ESCA spectrum of untreated silica indicated the presence of mainly Si, O, C (contamination), and trace amounts of F, N, Cu, and Na. Binding energies and atomic fractions of each element are given in Table V. Determined binding energies for Si 2p and O 1s were very close to the reported values for silica[53] of 102.5 and 531.7 eV, respectively. The surface of silica is relatively clean as evidenced by the very low concentration of trace elements.

The presence of F and Na were checked with ESCA on Iler treated silica and no trace of Na was detected. A small trace of F was seen. However, a trace of F was already present in untreated silica as seen in Table V.

Table IV. Binding energies and atomic fractions of C, Si and O in silica at various probe temperatures

	C		Si		O			
T	B.E.(eV)	A.F.	B.E.(eV)	A.F.	B.E.(eV)	A.F.	O/Si	C/Si
40°	284	0.298	153.3	0.191	531.9	0.510	2.67	1.55
100°	284	0.435	153.6	0.173	531.8	0.392	2.26	2.51
200°	284	0.442	153.5	0.171	531.8	0.387	2.26	2.59
300°	284	0.227	153.6	0.218	531.9	0.555	2.55	1.04
400°	284	0.166	153.6	0.232	532.0	0.602	2.59	0.714

Table V. ESCA analysis of silica

Element, core level	B.E.(eV)	A.F.
Si 2s	153.2	0.129
' $(2p^3)$	102.3	
O 1s	532.1	0.483
C 1s	284.0	0.388
F 1s	689.8	trace (0.0002)
N 1s	130.0	trace
Na Auger	263.8	trace
Cu Auger	73.5	trace

B. Adsorption of HCl

1. Isotherms: Adsorption and readsorption isotherms at 30°C of hydrogen chloride on silica outgassed at 100°, 200°, and 400°C are shown in Figures 6, 7, and 8, respectively. The number of moles of HCl adsorbed per unit area of silica surface (N^S) is plotted against the equilibrium pressure (P). The three sets of symbols represent three separate experimental runs. For easier observation of the outgas temperature (OGT) dependence, the above three adsorption isotherms are superimposed in Figure 9. As it is shown, with increasing outgas temperature, the hydrogen chloride adsorption at low equilibrium pressure increases whereas the hydrogen chloride adsorption decreases at higher equilibrium pressure. The observed dependence may be an indication of changes in the nature of the silica surface as a result of changes in the outgas temperature indicated by Boccuzzi, et al.[32]

In all cases, readsorption was lower than the original adsorption. This indicates that the adsorption process is not completely reversible; in other words, the adsorbed hydrogen chloride cannot be totally removed by evacuation at 30°C.

The reversibility of HCl adsorption was further studied by changing the outgas temperature before readsorption and this outgas temperature is termed the 're-outgas temperature' (ROGT). After the completion of the initial adsorption isotherm, the sample was reoutgassed at 100°, and at 400°C. Figure 10 shows the result of isotherms taken with silica originally outgassed at 100°C and

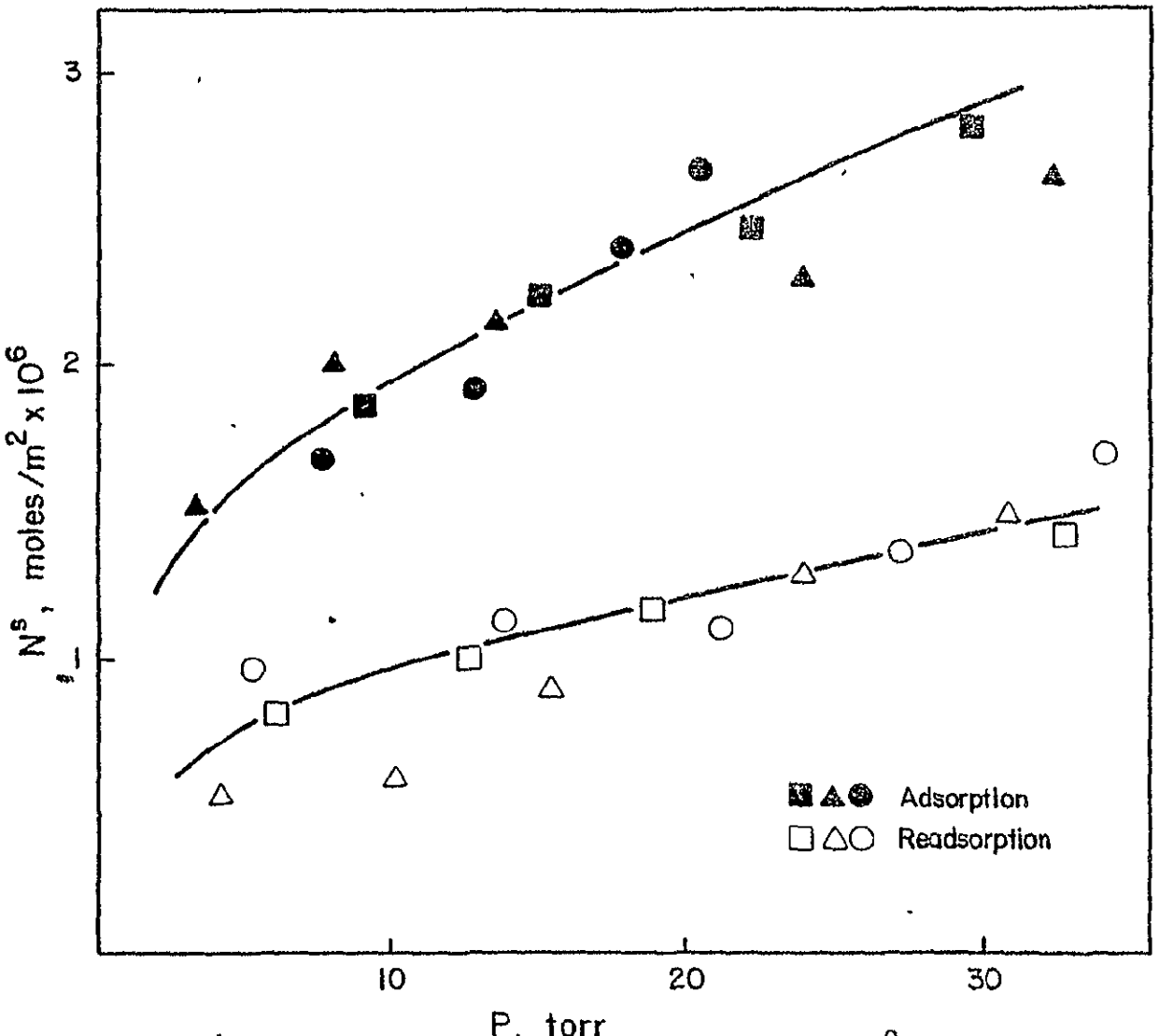

Figure 6. Adsorption and Readsorption isotherm at 30°C of HCl on Silica Outgassed at 100°C for 2 hours.

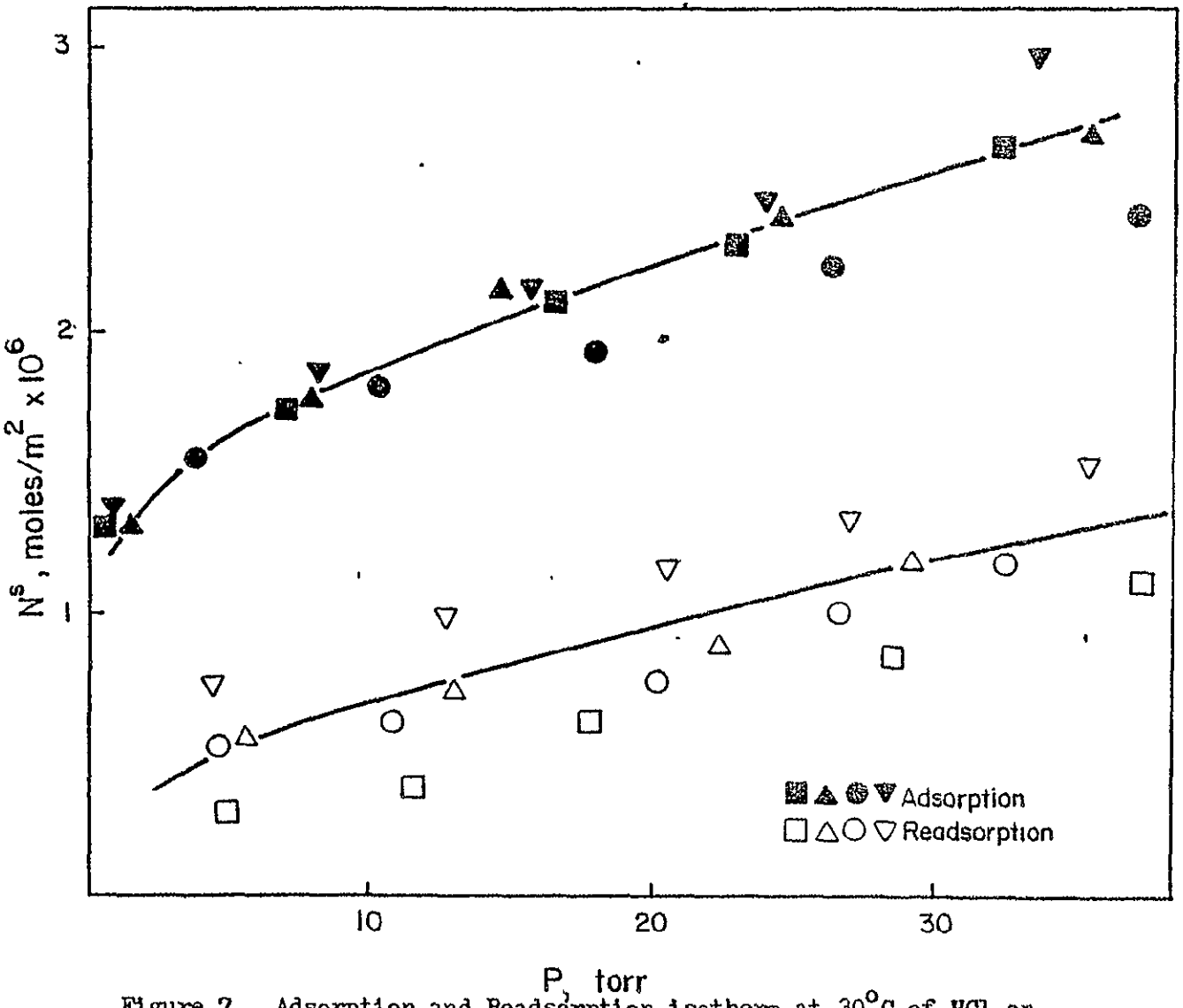

Figure 7. Adsorption and Readsorption isotherm at 30°C of HCl on Silica Outgassed at 200°C for 2 hours.

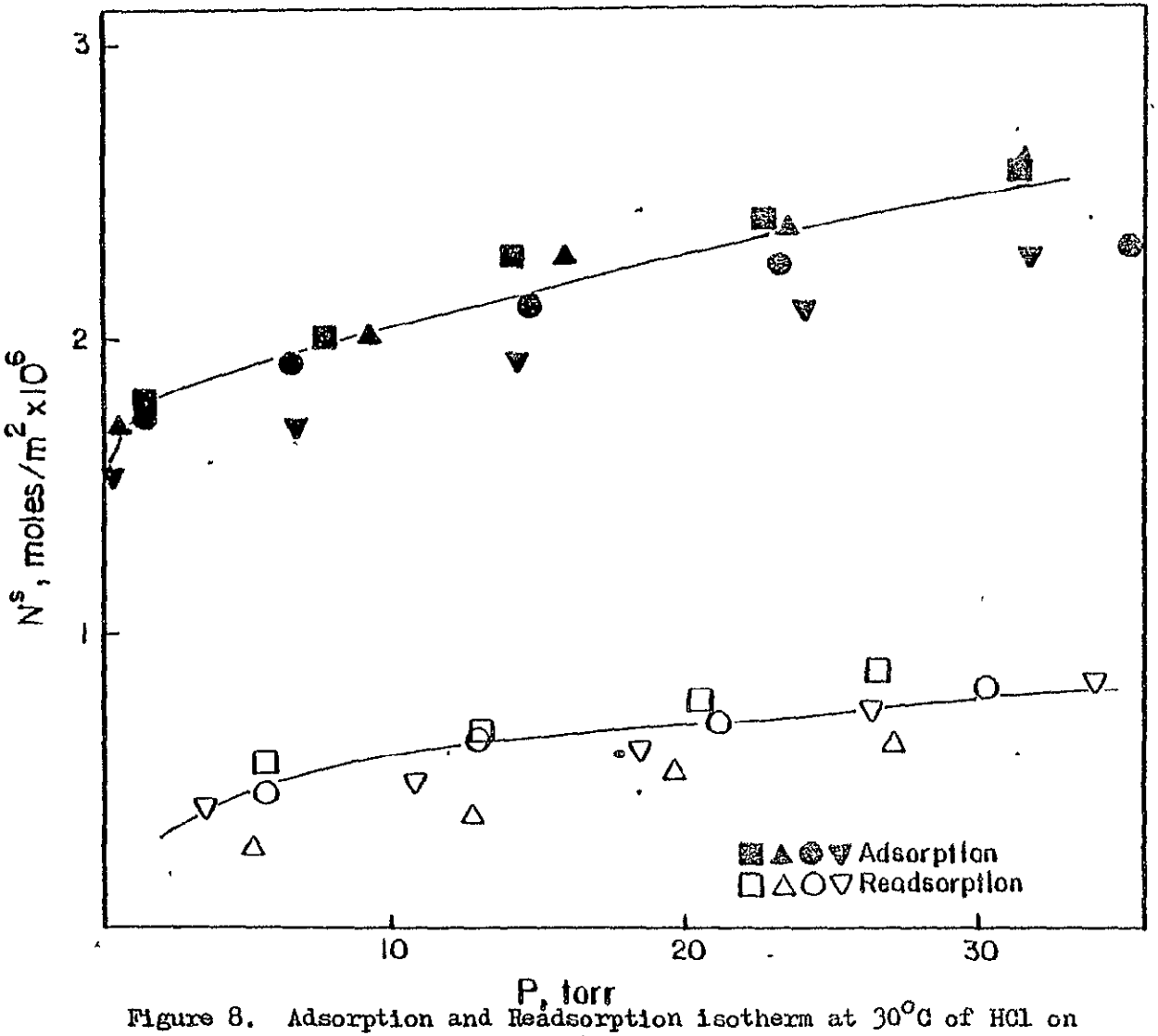

Figure 8. Adsorption and Readsorption isotherm at 30°C of HCl on Silica Outgassed at 400°C for 2 hours.

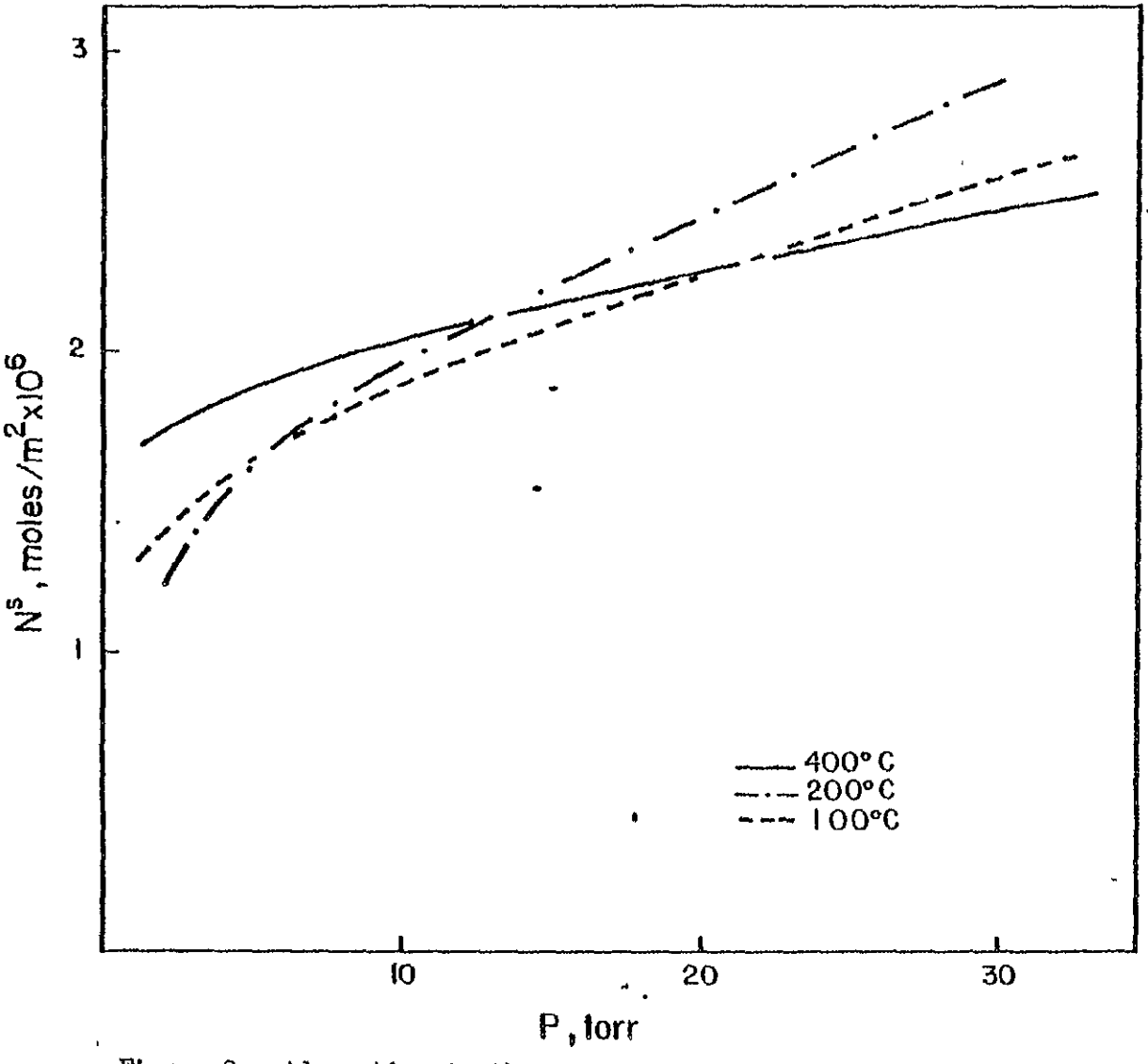

Figure 9. Adsorption isotherms at 30°C of HCl on Silica Outgassed at 100°C, 200°C, and 400°C.

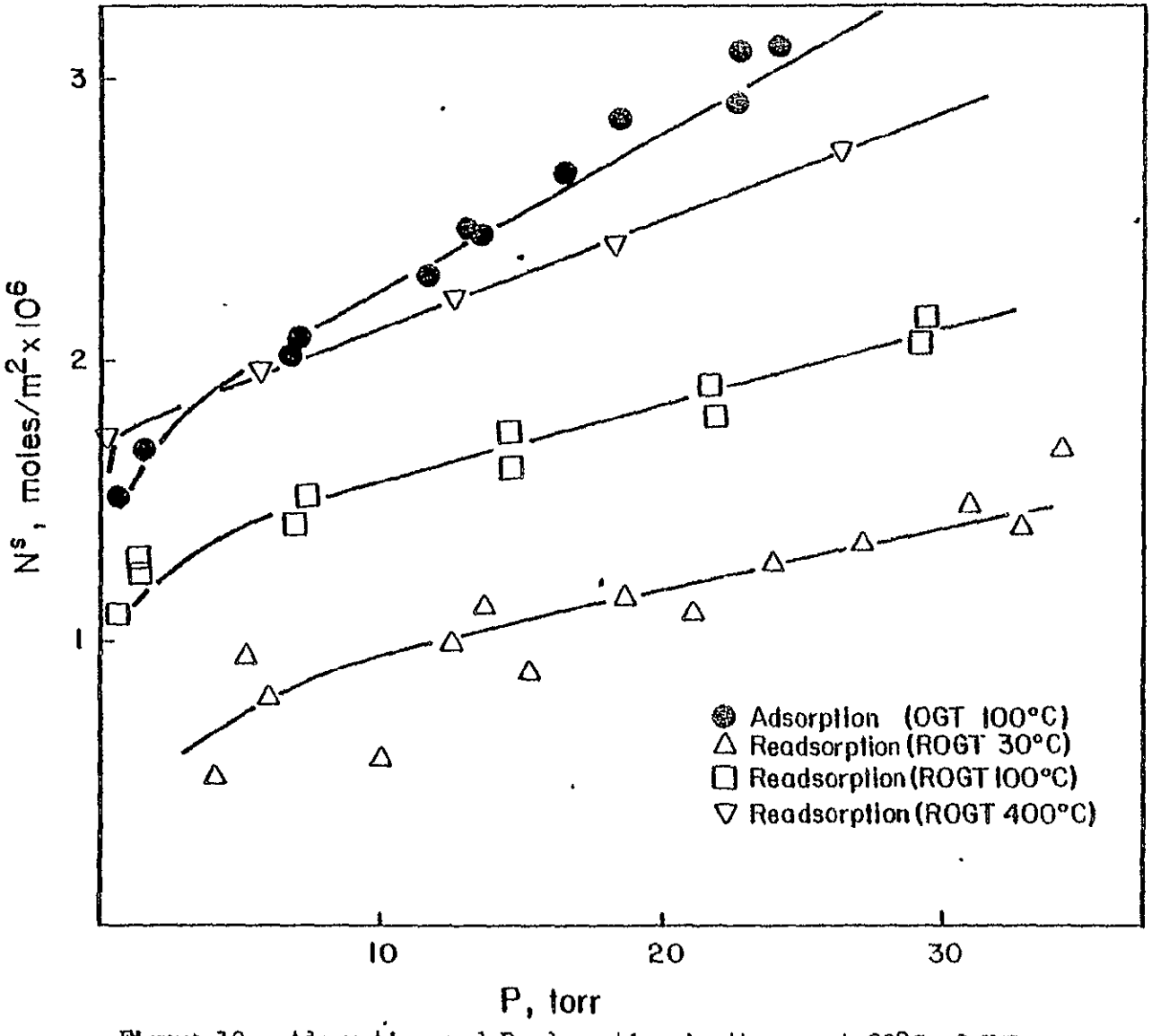

Figure 10. Adsorption and Readsorption Isotherms at 30°C of HCl on Silica Outgassed at 100°C and Reoutgassed at 30°, 100° and 400°C.

reoutgassed at 30°, 100°, and 400°C. Increasing amounts of hydrogen chloride were removed on reoutgassing at higher temperatures. In fact, the adsorption isotherm after reoutgassing at 400°C is nearly coincided with the original isotherm.

The next study involved isotherms taken with the original outgas temperature at 400°C and the reoutgas temperatures at 30°, 100°, and 400°C shown in Figure 11. Here, reoutgassing at 400°C made the overall adsorption/readsorption process a reversible one, i.e., adsorbed hydrogen chloride was totally removed by evacuation at 400°C. Brown and Hall[63] have used a 'comparison plot' which is an instructive way to compare isotherms. The total amount of hydrogen chloride adsorbed and readsorbed on silica at equal equilibrium pressures for three reoutgas temperatures are plotted against each other in Figure 12. The plots of adsorption of HCl on silica (OGT 400°C) reoutgassed at 100° and at 30°C versus on silica outgassed at 400°C indicated that not only the amount of HCl readsorption was less than the original HCl adsorption but also the two adsorption processes occurred on different types of surface; the lines do not go through the origin. However, the comparison plot (Figure 12) of adsorbed hydrogen chloride on silica (OGT 400°C) reoutgassed at 400°C versus on silica outgassed at 400°C is a straight line with zero intercept and a slope of 1.03. It is thus clear that the amount of adsorbed hydrogen chloride is the same for both adsorption and readsorption processes in this case. Of course, the same result is seen in Figure 11 but this comparative plot is a convenient, alternate way of presenting the data.

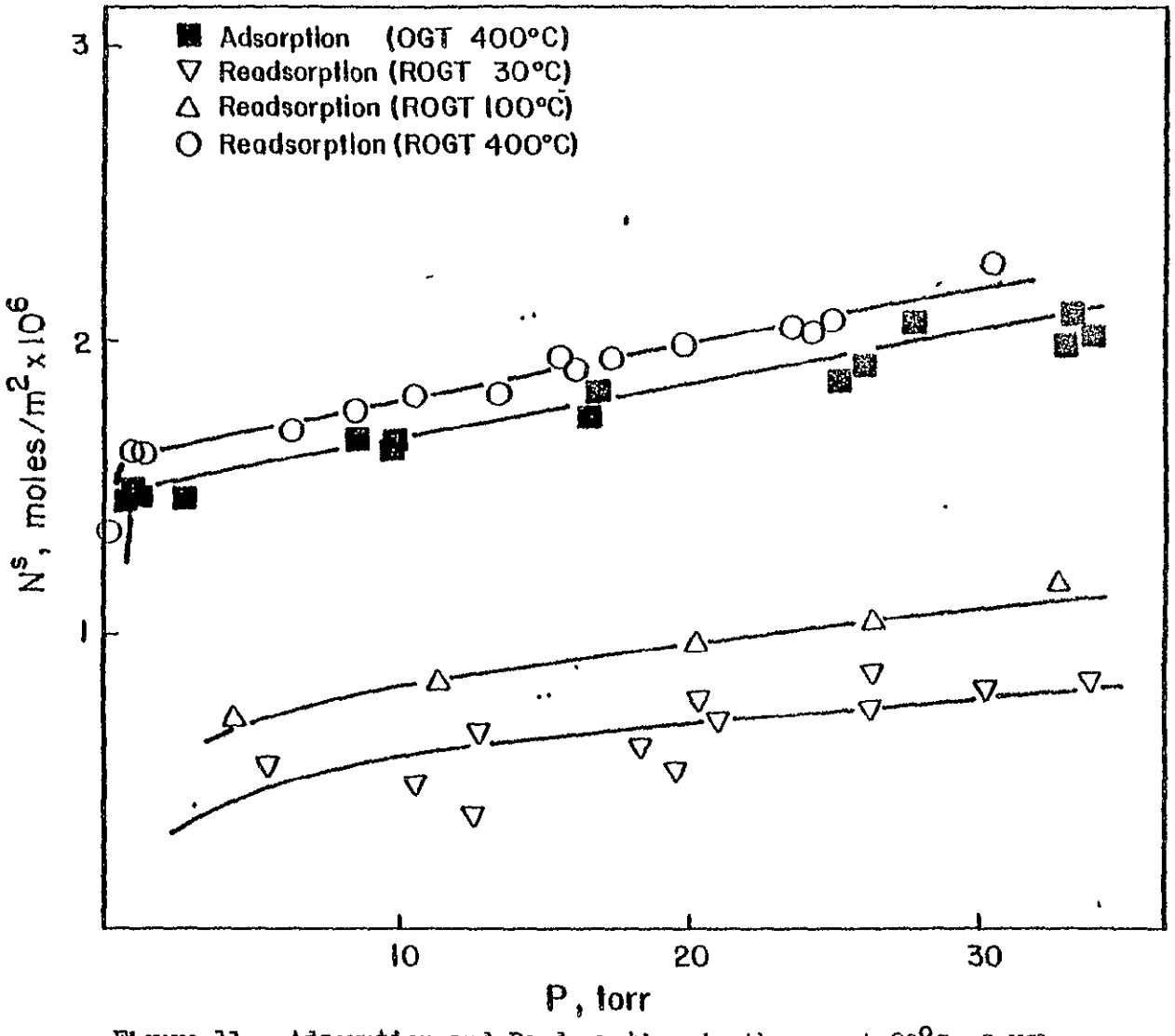

Figure 11. Adsorption and Readsorption isotherms at 30°C of HCl on Silica Outgassed at 400°C and Reoutgassed at 30°, 100° and 400°C.

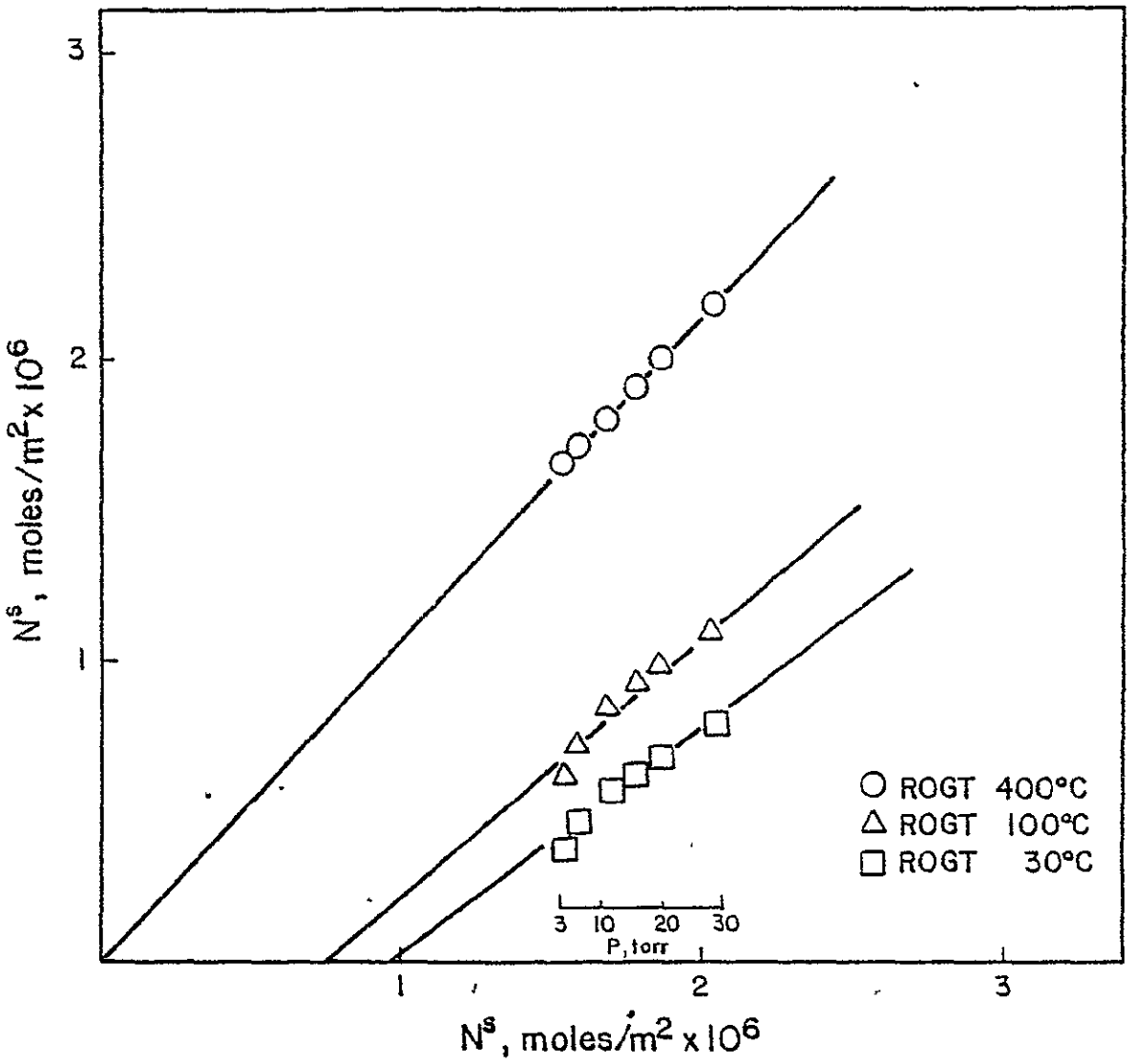

Figure 12. Comparison Plot of Total Amount of HCl Readsorbed vs Total Amount of HCl Adsorbed at 30°C on Silica Originally Outgassed at 400°C (Abcissa).

Blank runs were made to study the adsorption of hydrogen chloride on the empty sample bulb and adsorption was determined to be insignificant (~2.5% of the total adsorption) at low equilibrium pressures (<15 torr).

Adsorption isotherms of hydrogen chloride were taken at 30°C with Iler treated silica outgassed at 100°C for 2 hours and are shown in Figure 13. Again, evacuation at 30°C failed to remove all of the HCl adsorbed on the silica surface. A comparison plot of the adsorption isotherm data of Iler treated silica with that of untreated silica is given in Figure 14. Adsorption of HCl was higher on treated silica than on untreated silica. The higher adsorptivity of HCl on Iler treated silica might reflect changes in the surface energy after the etching process.

2. ESCA: ESCA analysis done on the silica after exposure to hydrogen chloride indicated the presence of chlorine. This is consistent with the result of the isotherm study where it was shown that a significant quantity of HCl remained on the surface after evacuation at 30°C (see Figure 6). Table VI shows the binding energies and relative atomic fractions of Si, O, and Cl present in each silica sample. The calculation of atomic fractions is only approximate and subject to criticism.[51] The figures in square brackets represents the number of samples employed in the averaging process. The fact that no significant shift in the binding energies occurred with increasing outgas temperature indicates that neither the oxidation state nor environment of species on the surface was

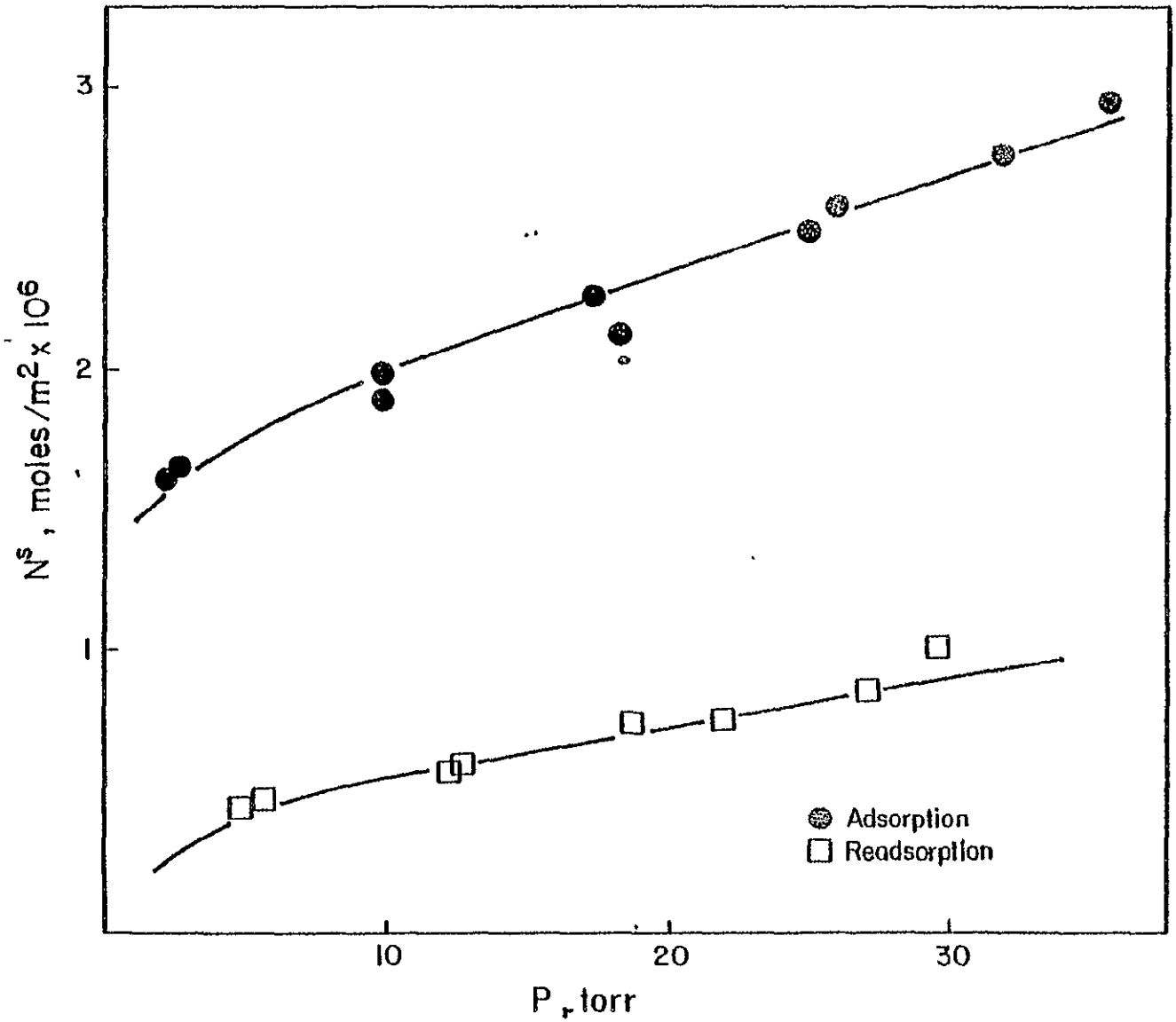

Figure 13. Adsorption and Readsorption at 30°C for HCl on Iler Treated Silica Outgassed at 100°C for 2 hours.

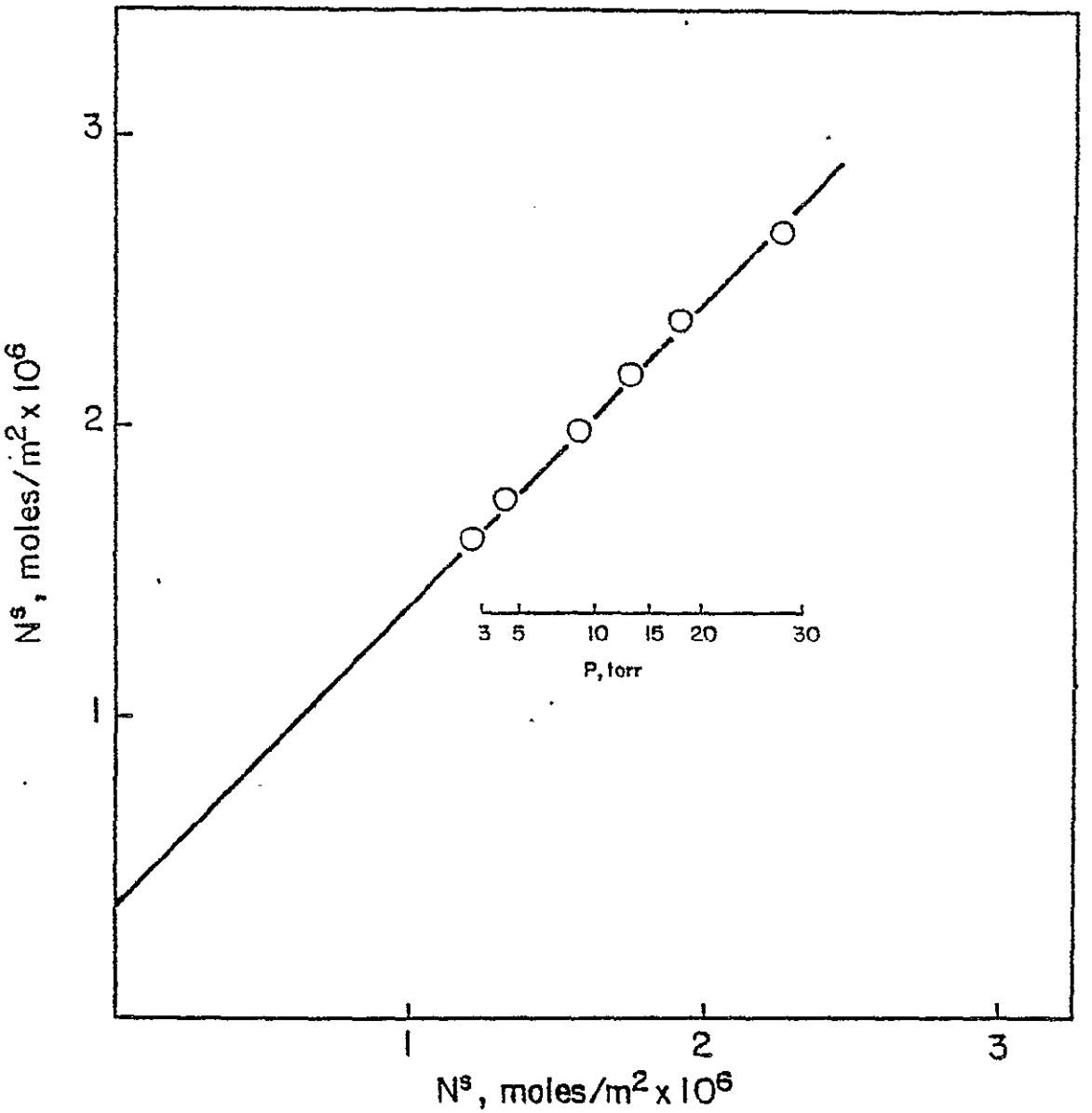

Figure 14. Comparison Plot of Adsorption of HCl at 30° on Iler Treated Silica Outgassed at 100°C for 2 hours vs on Untreated Silica Outgassed at 100°C for 2 Hours (Abcissa).

Table VI. ESCA analysis of silica exposed to HCl

OGT	Elements	B.E. (eV)	AF*	O/Si	Si/Cl
100°C	Si	153.2 ± 0.06 (0.04%)	0.213 ± 0.09 (4.2%)	2.7	48.4
[3]	O	531.7 ± 0.25 (0.05%)	0.581 ± 0.028 (4.8%)		
	Cl	198.0 ± 0.06 (0.03%)	0.00440 ± 0.00071 (16.1%)		
200°C	Si	153.3 ± 0.082 (0.05%)	0.219 ± 0.006 (2.7%)	2.6	50.1
[4]	O	531.7 ± 0.05 (0.01%)	0.568 ± 0.011 (1.9%)		
	Cl	198.0 ± 0.29 (0.15%)	0.00437 ± 0.00097 (22.2%)		
400°C	Si	153.3 ± 0.17 (0.11%)	0.198 ± 0.027 (13.6%)	2.8	80.8
[4]	O	531.8 ± 0.13 (0.02%)	0.552 ± 0.025 (4.5%)		
	Cl	198.6 ± 0.71 (0.35%)	0.00245 ± 0.00143 (59.1%)		

*Carbon accounts for the balance

influenced much by the outgas temperature. A relatively constant value of O/Si ratio was observed and the value was again greater than 2. An additional comment should be added in regard to the values of Si/Cl ratio. Due to relatively small intensities of 'Cl' peak, high standard deviation was found in the atomic fraction of Cl. Thus, the variation in the value of Si/Cl ratio may be a result of such problems.

The results of the angular probe analysis are given in Table VII. Although the elemental intensities decreased with the decrease in take-off angle (from 90° to 11°), the value of the ratio of Si to Cl or O to Cl also decreased. Thus, Cl is assumed to be present on the surface and not distributed throughout the sampling region (~100 Å). Once again, the values of Si/O ratio remained relatively constant. An unexplained inverse trend in the Si/Cl and O/Cl ratio was observed with the 6° probe.

The results of ESCA analysis done on the Iler treated silica after the reaction with hydrogen chloride are given in Table VIII. The binding energies were not as reproducible compared to those obtained from the untreated silica. However, the binding energies of Si, O, and Cl in both treated and untreated silica were approximately the same. The value of O/Si ratio was also reasonably close to the value of untreated silica. A problem with intensities of 'Cl' peak was again present in the value of Si/Cl ratio. The detection of chlorine further supports the results of isotherm study.

The binding energy for every Cl 2p composite photopeak was about 198.0 eV. This value compares favorable with that for chloride

Table VII. Results of ESCA analysis on silica exposed to HCl taken at take-off angles of 90°, 30°, 11°, and 6°.

	Si		O		Cl				
Angle	B.E.(eV)	A.F.	B.E.(eV)	A.F.	B.E.(eV)	A.F.	Si/Cl	O/Cl	O/Si
90°	153.3	0.217	531.7	0.579	198.4	0.00317	68.45	182.6	2.67
30°	153.4	0.226	531.8	0.588	198.1	0.00454	49.78	129.5	2.60
11°	153.4	0.229	531.8	0.567	198.3	0.00509	44.99	111.4	2.48
6°	153.4	0.204	531.8	0.534	199.0	0.00455	45.49	117.4	2.62

Table VIII. ESCA analysis on Iler treated silica exposed to HCl

Elements	B.E.(eV)	A.F.	O/Si	Si/Cl
Cl	197.1 ± 0.9	0.00606 ± 0.00122	2.43	34.0
O	532.8 ± 1.1	0.501 ± 0.182		
Si	153.8 ± 0.6	0.206 ± 0.070		
C	284	0.289 ± 0.251		

ion in simple inorganic salts.[53,64] Indeed, the binding energy of the same Cl photo peak obtained for the HCl/Al_2O_3 system was also 198.0 eV.[65]

3. SEM/EDAX: SEM photomicrographs were taken for untreated silica before and after adsorption of HCl. A photomicrograph of untreated silica is shown in Figure 15 and shows clusters rather than primary particles. There was no apparent difference in the SEM photomicrograph after exposure of silica to HCl. EDAX analysis indicated no trace of Cl on the surface of silica after the exposure to HCl. This result does not contradict the results of ESCA analysis above since SEM/EDAX is more of a bulk analysis rather than a surface analysis technique.

SEM photomicrographs on Iler treated silica were very similar to the ones of untreated silica. This similarity does not imply that the two silica samples, treated and untreated, have the primary particles of the equal size. Rather, the difference in the sizes of the primary particles was not detected. EDAX analysis was done on Iler treated silica after exposure to HCl and again Cl was not detected.

4. Infrared spectroscopy: The infrared spectrum of untreated silica was taken in the region between 4000 and 200 cm^{-1} and shown in Figure 16. The spectrum matched very well with the spectrum of quartz reported in the literature.[66] The OH band (3800 - 3500 cm^{-1}) could not be detected due to the very low surface area of the sample. A small OH band was observed, however, on ordinate expansion (x10)

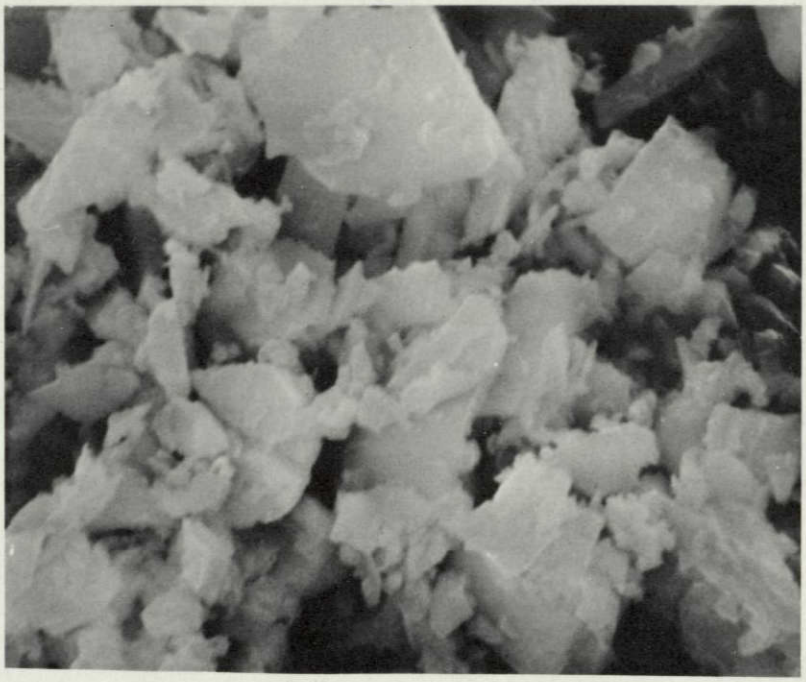

Figure 15. SEM photomicrograph of Min-U-Sil 5 (x2000).

in the 4000 - 3600 cm^{-1} region and the spectrum is also shown in Figure 16. The Si-Cl absorption band was not observed in the 640 - 425 cm^{-1} and 250 - 200 cm^{-1} regions.

5. Calorimetry: The heat of immersion of silica increased with increasing HCl concentration as shown in Table IX. This trend is consistent with the work of Tschapek, et al.[54] who reported the heat of immersion of aerosil outgassed at 110°C in 0.001, 0.01, and 0.1 N HCl (aq) as 154, 158, and 171 mJ/m^2, respectively. Whalen reported the heat of immersion of quartz (<5μ particles) in water as a function of pretreatment temperature.[35] The reported values for heats of immersion of quartz outgassed at 100°, 200°, and 400°C were 330, 375, and 370 mJ/m^2, respectively. These values are all lower than the ones obtained for 0.001 N HCl as shown in Table IX.

Heats of immersion of Iler treated silica in hydrochloric acid solution of varying concentration are also listed in Table IX. Again, there was a general trend of increasing heats of immersion with higher acid concentration. It was interesting that although the heats of immersion were lower with Iler treated silica than untreated silica, the adsorption of HCl was greater on Iler treated silica than on untreated silica (see Figure 14).

The heat evolved due to the process of empty bulb breaking was measured 4 times and was found to be 96 ± 24 mJ. All heats reported in Table IX have been corrected for heat of empty bulb breaking.

Table IX. Heats of Immersion of Silica in Aqueous HCl

	OGT			Iler treated silica
HCl Conc.	100°C(mJ/m^2)	200°C(mJ/m^2)	400°C(mJ/m^2)	OGT 100°C(mJ/m^2)
0.1N	519.5 ± 19.4	558.1 ± 39.8	951.7 ± 8.3	266.6 ± 18.5
0.01N	402.2 ± 16.2	506.3 ± 12.0	641.7 ± 31.2	179.3 ± 103.1
0.001N	345.5 ± 45.1	439.8 ± 25.0	537.9 ± 53.6	170.3 ± 84.2

PART II. NASA SAMPLES

A. Characterization

1. Surface area: The two ground debris samples NASA #2 and #4 had surface areas of 0.35 and 0.13 m^2/g, respectively. These values are much lower than for the model silica, Min-U-Sil 5 (particle size $\leq 5\mu$), with a surface area of 5.06 m^2/g. This implies that NASA samples are of larger particle size than silica. Indeed, the analysis of NASA #2 sample tabulated in Table X shows that 96% of the total sample is sand whose particle size is $<50\mu$.

2. ESCA: Wide scan ESCA spectra on NASA #2 and NASA #4 were taken. The spectra showed the presence of a variety of elements on the surface. Table XI shows the results of the analysis. Both samples showed trace amounts of Cl. The binding energy of the Cl photopeak agreed with that of the chloride ion. The values of O/Si ratio indicatethat oxygen in the NASA samples is not just from silica (O/Si ~ 2) but also from some other oxycompounds such as CaOH, Al_2O_3, etc. It was interesting that Cu and Al were detected only in NASA #4, the sample collected furtherest from the launch pad.

Compared to ESCA analysis, the results of nuclear activation analysis (NAA) shown in Table XII indicated the presence of many more elements and in some cases, the results of the two analysis did not agree. However, this difference may be anticipated due to the difference in the nature of the two techniques: ESCA is a surface technique and NAA gives a bulk analysis. An additional unexpected NAA result was the absence of Si in the NASA samples.

Table X. Fractionation analysis and Mineralogy of Sand Fraction of NASA #2

Fraction	Size Range	%
Organic Matter		0.53
Clay	2	0.04
Silt	50 - 2	1.01
Very Fine Sand	105 - 50	1.79
Fine Sand	250 - 105	32.86
Medium Sand	500 - 250	51.97
Coarse Sand	1000 - 500	11.03
Very Coarse Sand	1000	0.77

The most active fraction is the organic matter and clay. The clay is composed of 2:1 interstratified minerals such as kaolinite, gibbsite and quartz.

Mineralogy of Sand Fraction

500 - 250	Quartz:	88%
	Mica:	5%
	Heavy Minerals:	6%
105 - 50	Quartz:	60%
	Feldspar:	6%
	Mica:	2%
	Heavy Minerals:	32%

Heavy minerals are minerals with specific gravity greater than 2.86. They include Eipdote, Hornblende, Zircon, Apatite, Tourmaline, Magnetite and Ilmenite.

Table XI. Wide Scan ESCA analysis of NASA #2 and NASA #4

	NASA #2		NASA #4	
Elements	B.E.	A.F.	B.E.	A.F.
O	531.6	0.192	531.8	0.380
Cu			110.0	0.0114
Ca	346.7	0.0160	347.1	0.00848
C	284.0	0.728	284.0	0.529
N	398.4	0.0158	399.5	0.0115
Si	153.1	0.0358	153.1	0.0430
Cl	197.6	0.0125	198.2	0.00490
Al			118.7	0.0119
O/Si	5.36		8.84	
Si/Cl	2.86		8.78	

Table XII. Neutron Activation Analyses of NASA #2 and NASA #4

Element	Conc. in #2, ppm (g/g)	Conc. in #4, ppm (g/g)
Al	1810.	1790.
Ca	63700.	20500.
Cl	86.	-
Fe	1940.	1410.
K	292.	292.
Mg	1091.	489.
Na	.659.	410.
Sr	358.	146.
Ti	631.	155.

Overall, significant elemental surface heterogeneity was observed with the NASA samples compared to the relatively clean silica surface.

Samples from the launch pad itself before and after a launch were also supplied by NASA. Wide scan ESCA analysis were done on the pre and post launch samples and the results are tabulated in Table XIII. A relatively low atomic fraction was observed for Si in both samples and the two samples showed the presence of identical elements.

3. SEM/EDAX: No apparent difference was noticed between NASA #2 and NASA #4 in the SEM photomicrographs of the two samples as shown in Figures 17 and 18, respectively. Larger particle sizes observed were consistent with lower surface areas when compared to silica (Min-U-Sil). EDAX analysis indicated the presence of Si and Ca in both NASA #2 and NASA #4. However, Al was detected only in NASA #4 consistent with the ESCA analysis.

A careful observation of the SEM photomicrographs of the pre and post launch samples revealed an interesting difference as shown in Figures 19, and 20, respectively. Small and almost perfectly spherical particles were seen only in the post launch sample (see Figure 20). EDAX analysis of these small particles indicated high concentrations of Al as shown in the spectrum in Figure 21. Dillard, Seals and Wightman[67] observed similar spherical particles in the SEM/EDAX analysis of samples collected in the exhaust cloud. Again, high aluminum concentrations were noted in the EDAX spectrum.

Table XIII. Wide Scan ESCA analysis of pre launch and post launch samples taken from the launch pad

	Pre Launch		Post Launch	
Elements	B.E.(eV)	A.F.	B.E.(eV)	A.F.
C	284.0	0.739	284.0	0.629
Si	153.2	0.0359	153.0	0.0685
O	532.0	0.174	531.3	0.224
Cl	198.0	0.0113	200.1	0.0341
N	398.8	0.00683	399.0	0.00753
Al	119.0	0.0222	118.5	0.0268
Ca	346.8	0.00999	347.0	0.0108

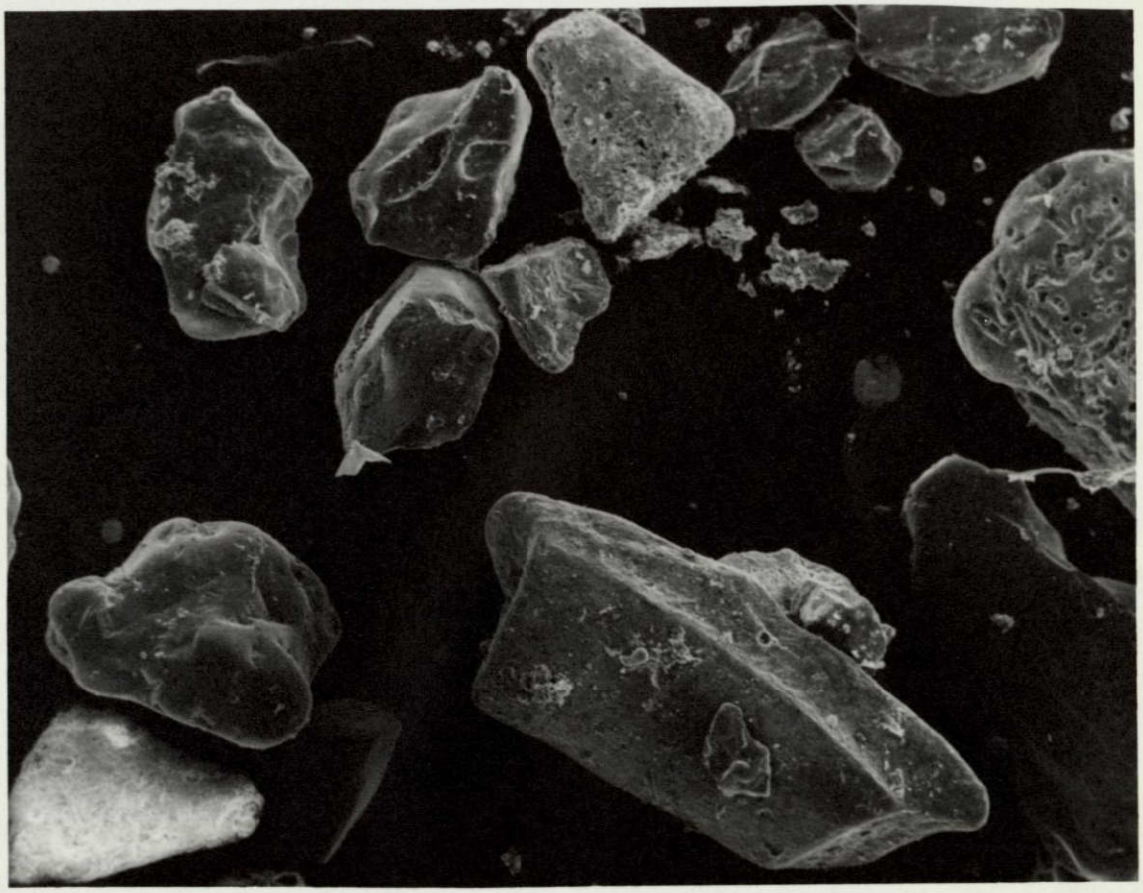

Figure 17. SEM photomicrograph of NASA #2 (x50).

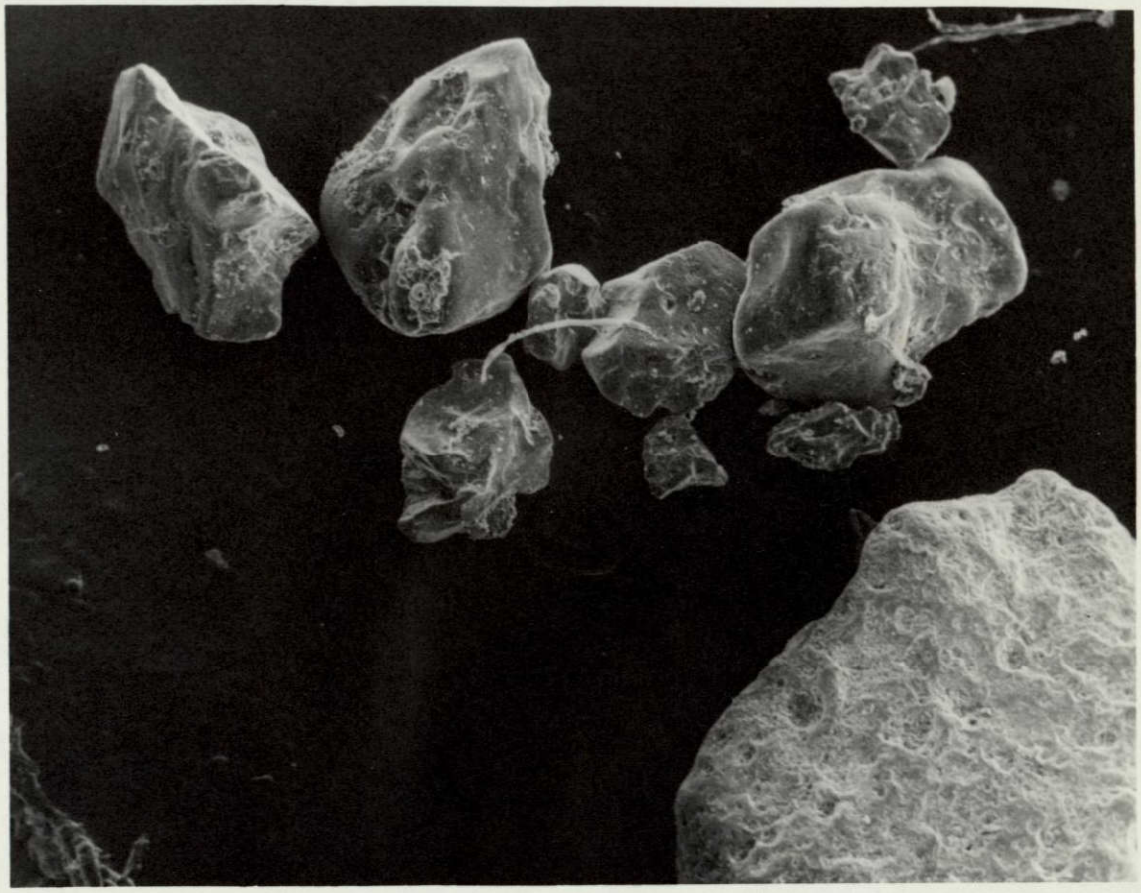

Figure 18. SEM photomicrograph of NASA #4 (x50).

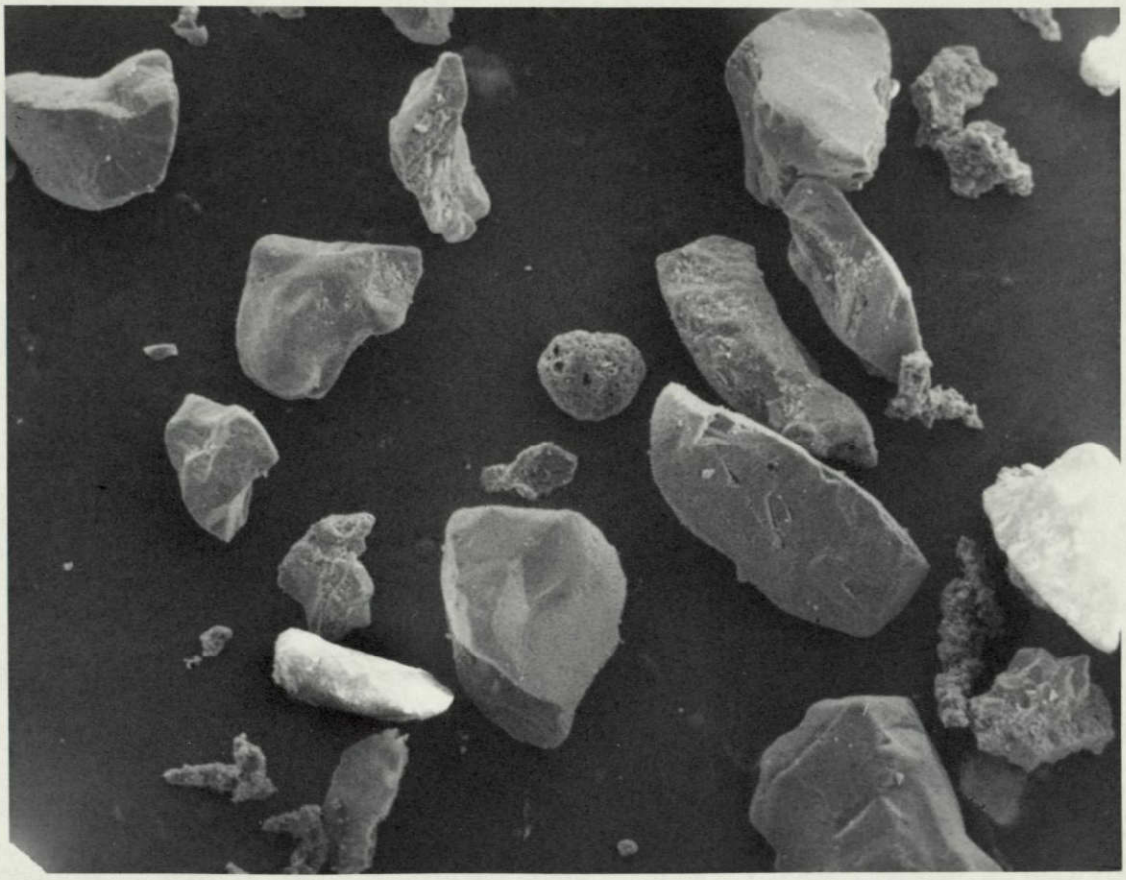

Figure 19. SEM photomicrograph of pre launch pad sample (x100).

ORIGINAL PAGE IS
OF POOR QUALITY

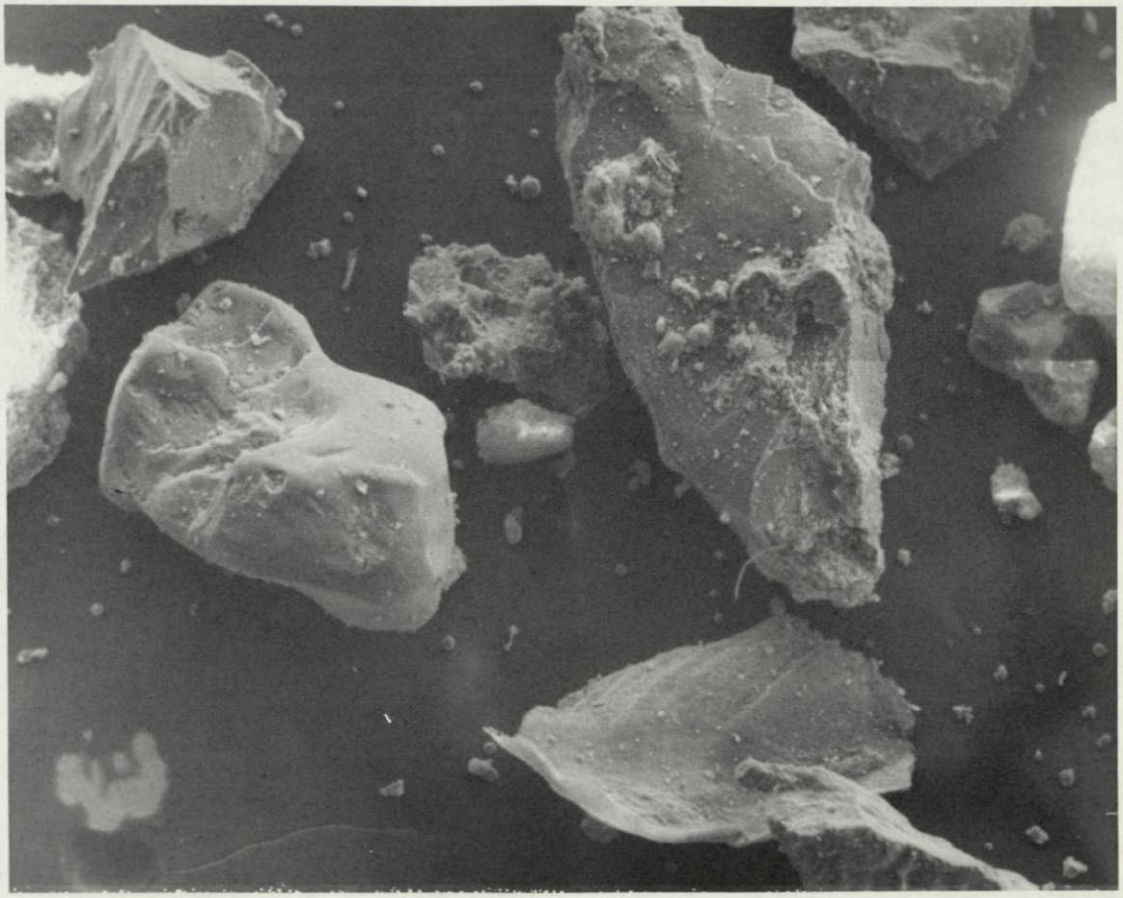

Figure 20. SEM photomicrograph of post launch pad sample (x100).

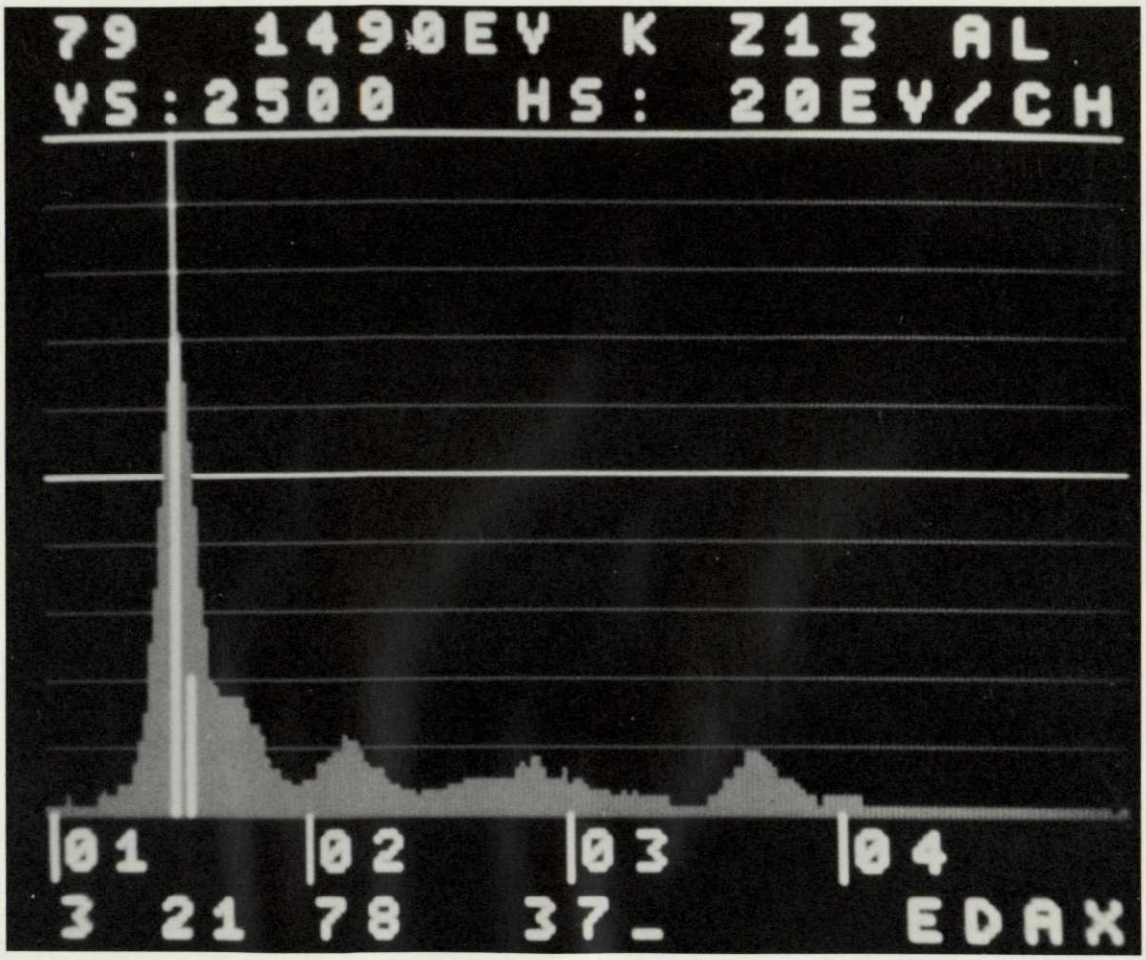

Figure 21. EDAX of spherical particles observed in post launch pad sample.

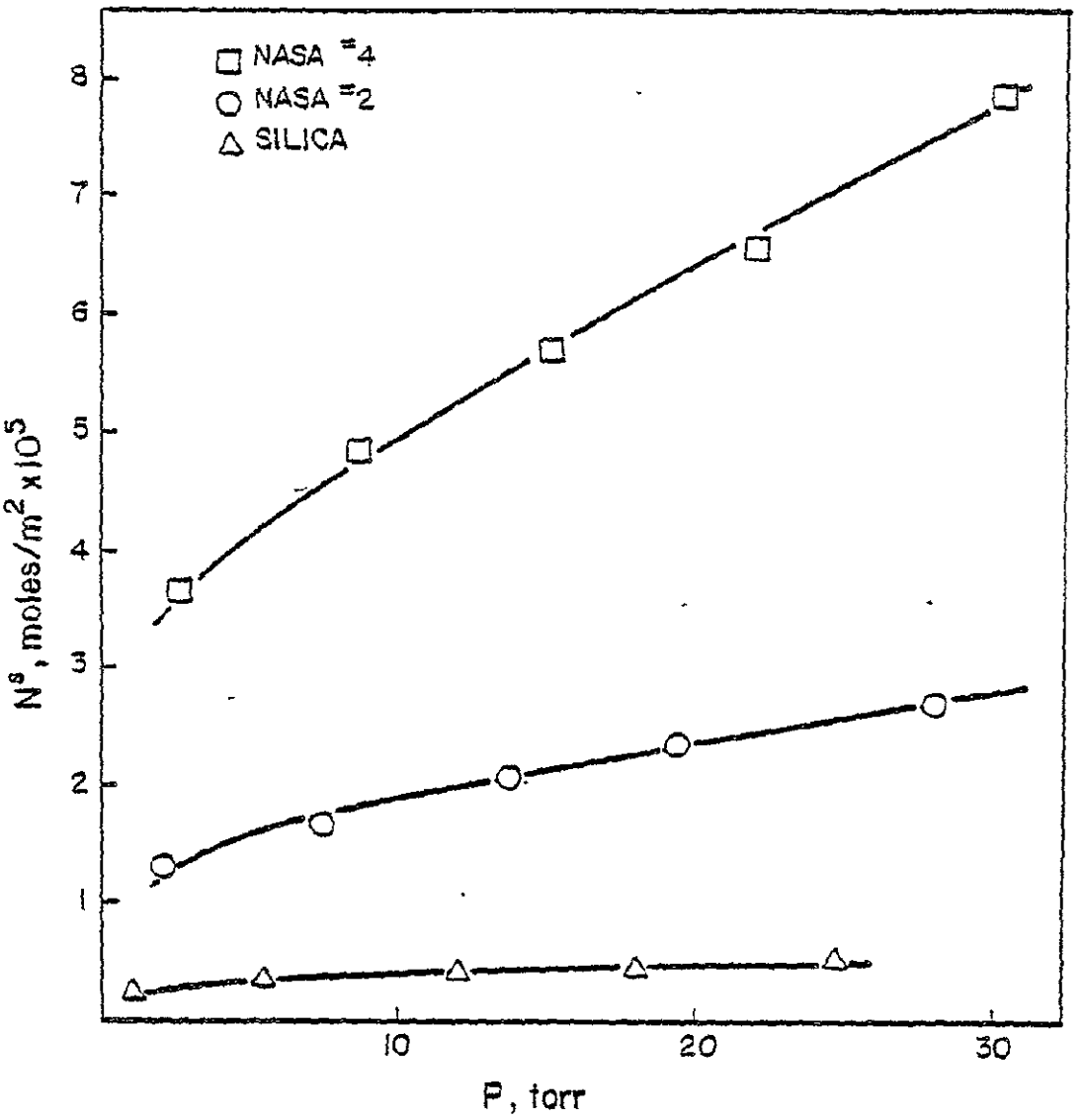

Figure 22. Adsorption isotherm at 30°C of HCl adsorbed on NASA #4, NASA #2, and silica outgassed at 100°C for 2 hours.

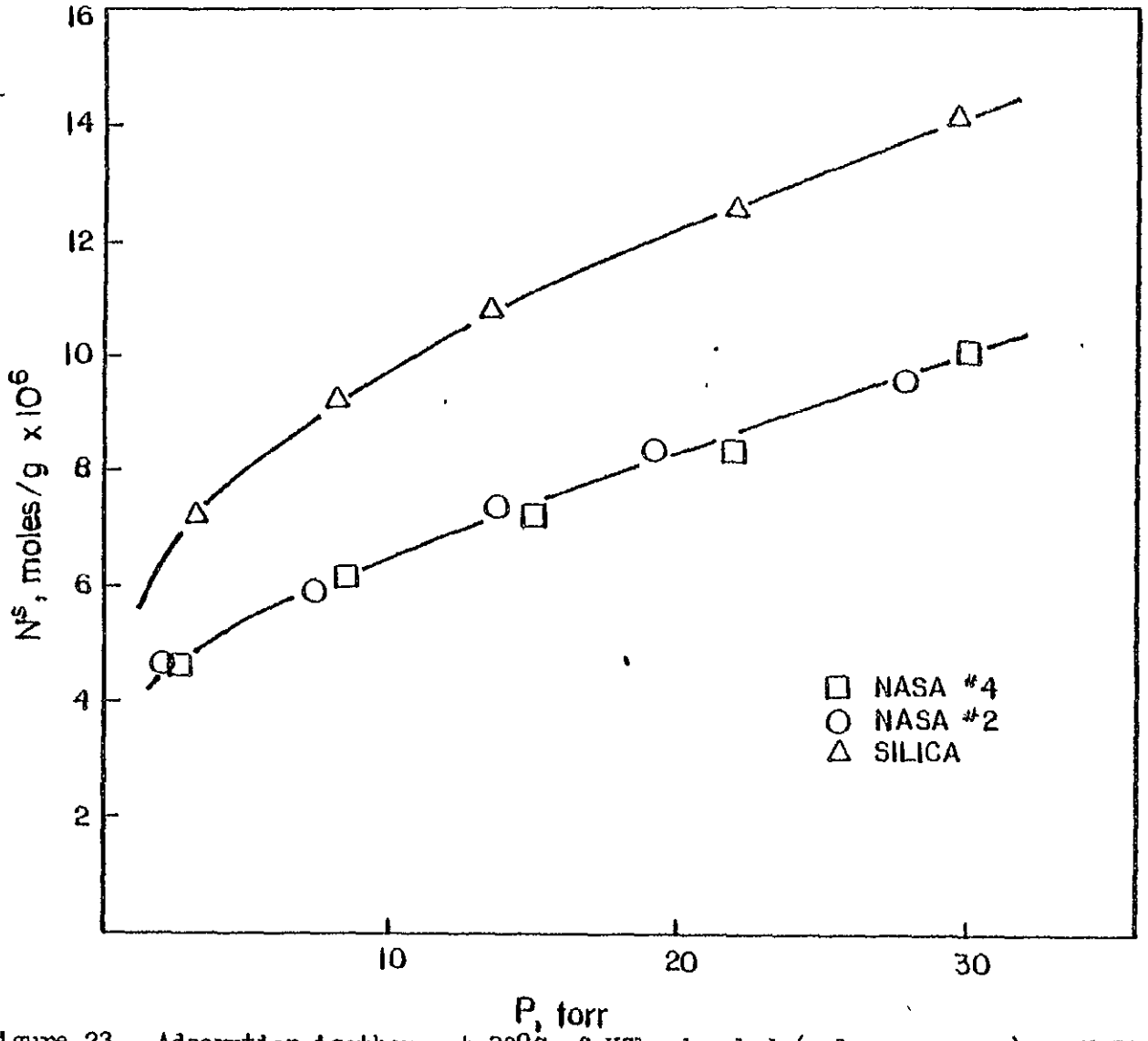

Figure 23. Adsorption isotherm at 30°C of HCl adsorbed (moles per gram) on NASA #4, NASA #2, and silica outgassed at 100°C for 2 hours.

Table XIV. Binding energies and atomic fraction (A.F.) of C, Si, O, and Cl in NASA #2 and #4 after exposure to HCl.

	C		Si		O		Cl			
	B.E.(eV)	A.F.	B.E.(eV)	A.F.	B.E.(eV)	A.F.	B.E.(eV)	A.F.	O/Si	Si/Cl
NASA #2	284.0	0.433	153.0	0.085	531.6	0.462	197.8	0.019	5.45	4.47
NASA #4	284.0	0.538	153.0	0.0774	531.5	0.370	197.2	0.0149	4.78	5.19

measured Cl concentration was about 4 times higher for the NASA samples after HCl exposure than for silica. This is despite the fact that measured Si concentration was about one-third lower for the NASA samples than for silica (see Table VI). This is consistent with the result of the isotherm measurements that HCl interacts with greater affinity with some component in the NASA samples other than silica. It should be noted, however, that 'Cl' was observed in NASA samples before the HCl exposure. The value of Si/Cl ratio did decrease in NASA #4. The reverse trend in the NASA #2 sample might be due to the heterogeneity of the sample batch.

V. CONCLUSIONS

The following conclusions were derived from a study of the interaction of hydrogen chloride with silica (α quartz):

1. Adsorption at 30°C of HCl on microcrystalline silica outgassed at 100°, 200°, and 400°C showed a minimal dependence on the outgas temperature.
2. Adsorption of HCl at 30°C was about 40% reversible when silica was reoutgassed at 30°C. However, adsorption was completely reversible when silica was reoutgassed at 400°C.
3. Etching the silica surface with 10% HF decreased the surface area by 40%. Adsorption of HCl on etched silica was still found to be only partially reversible at 30°C.
4. ESCA analysis showed the presence of chloride ion on the silica surface supporting the results of the isotherm study. An angular probe study revealed that the adsorbed chloride ion was localized on the surface and did not diffuse into the entire sampling region (~ 100 Å).
5. Heats of immersion of silica in aqueous HCl solutions increased with increasing outgas temperature and with increasing acid concentration.
6. NASA ground debris samples showed much greater adsorption of HCl than silica. ESCA analysis further supported this with greater chloride intensities.

7. Comparison of the results of SEM/EDAX analysis of the post and pre launch pad samples showed the presence of spherical aluminum particle only in the post launch sample.

REFERENCES

1. Bean, S.L.; Wall, H. Jr. Nat'l. Air Pollut. Control Adm. (U.S.), Publ., AP Ser; Washington, D.C.; AP-54, 1969.

2. Tokyo Metropolitan Government, Japan. Public Nuisance Control Division. Kogai to Taisaku 1966, 2 (7) 461-6; APTIC 16521; Chem. Abstr. 1972, 76, B27758J.

3. Scharfenstein, Otto H.C., Stadtehygiene, 1969, 20(8), 192-6; Chem. Abstr. 1969, 71, 116261f.

4. Shriner, D.S.; Lacasse, N.L. Phytopathology 1972, 62, 427-9.

5. Grieser, N. Jahresber.-Med. Inst. Lufthyg. Silikoseforsch, 1972, 64-8. Chem. Abstr. 1976, 84, R64630x.

6. Wogrolly, E.; Strauss, W.; Schmitz, E. Oesterr. Tunstst Z. 1973, 5(5/6) 80; Chem. Abstr. 1974, 81, 110814y.

7. Spence, J.W.; Hanst, P.L.; Gay, B.W., Jr. Air Pollut. Control Assoc. 1976, 26, 994-6.

8. NASA JPL Publication 77-9; California, 1977.

9. L. Zelazny. Private communication, 1977.

10. Gregg, S.J.; Sing, K.S.W. "Adsorption, Surface Area and Porosity;" Academic Press: New York, 1967.

11. Flood, E.A., Ed. "The Solid Gas Interface;" Marcel Dekker, Inc.: New York, 1967.

12. Schulman, J.H., Ed. "Solid/Gas Interface. Second International Congress of Surface Activity, II;" Academic Press, Inc.: New York, 1957.

13. Park, C. Atmos. Environ. 1976, 10, 693-702.

14. Bailey, R.R. Ph.D. Dissertation, Virginia Polytechnic Institute and State University, Blacksburg, Virginia, 1976.

15. Cofer, W.R., III; Pellet, G.L. NASA Technical Paper 1105; Washington, D.C., 1978.

16. Iler, R.K. "The Colloid Chemistry of Silica and Silicates;" Cornell University Press: Ithaca, 1955.

17. Sosman, R.B. "The Properties of Silica," ACS Monograph 37; Chemical Catalogue: New York, 1927.

18. Sosman, R.B. "The Phases of Silica;" Rutgers University Press: New Brunswick, 1965.

19. Levin, E.M.; Robbin, C.R.; McMurdie, H.F. "Phase Diagram for Ceramists;" American Ceramic Society: Columbus, Ohio, 1961.

20. Mellor, J.W.; "Comprehensive Treaties on Inorganic and Theoretical Chemistry." Vol. VI, Wiley.

21. Iler, R.K. "The Colloid Chemistry of Silica and Silicates;" Cornell University Press: Ithaca, New York, 1955; p 5.

22. Mellor, J.W.; "Comprehensive Treaties on Inorganic and Theoretical Chemistry", Vol. VI; Longmans, Green & Co.: London, 1925; pg 274.

23. Ibid., pg. 249.

24. Hair, M.L. "Infrared Spectroscopy in Surface Chemistry;" Marcel Dekker, Inc.; New York, 1967; Chapter 4.

25. Kiselev, A.V.; Lygin, V.I. "Infrared Spectra of Surface Compounds;" Halsted Press; New York,. 1975. Chapters 4-7.

26. Snyder, L.R. "Principles of Adsorption Chromatography;" Marcel Dekker, Inc.: New York, 1968; p. 156-81.

27. Davydov, V. Ya.; Kiselev, A.V.; Zhuravlev, L.T.; Trans Faraday Soc., 1964, 60, 2254-63.

28. Hambleton, F.H.; Hockey, J.A.; Trans. Faraday Soc., 1966, 62 1694-1701.

29. Davydov, V.Ya; Zhuravlev, L.T.; Kiselev, A.V. Russ. J. Phys. Chem. (Engl. Transl.) 1964, 38 1108-1112.

30. Young, G.J. J. Colloid Sci., 1958, 13, 67.

31. Hair, M.L. "Infrared Spectroscopy in Surface Chemistry;" Marcel Dekker, Inc.: New York, 1967; p. 87.

32. Boccuzzi, F.; Coluccia, S.; Ghiotti, G.; Morterra, C.; Zecchina, A. J. Phys. Chem. 1978, 82, 1298-1303.

33. Basila, M.R. J. Chem. Phys. 1961, 35, 1151.

34. Hair, M.L; Hertl, W. J. Phys. Chem. 1969, 73, 4269-76.

35. Whalen, J.W. Advances in Chemistry, 1961, 33, 281-90.

36. De Boer, J.H.; Vleeskens, J.M. Proc. Kon. Ned. Akad. v. Wetensch. Ser. B. 1958, B61, 2-11.

37. Boehm, H.P. Angew. Chem. 1966, 5, 533.

38. Fripiat, J.J.; Uytterhoeven, J.B. J. Phys. Chem. 1962, 60, 300.

39. Wagner, B.E.; Helbert, J.N.; Poindexter, E.H. Surface Sci. 1977, 67, 251-268.

40. Iler, R.K. "The Colloid Chemistry of Silica and Silicates;" Cornell University Press: Ithaca, New York, 1955; p. 242.

41. Zhuravlev, L.T.; Kiselev, A.V. Symp. Surface Area Determination 1970, Butterworths.

42. Surface Chemistry of Oxides, Discuss. Faraday Soc., 1971, 52.

43. Boonstra, A.H.; Mutsaers, C.H.H.A. J. Phys. Chem. 1975, 79, 1694.

44. Tyree, S.Y., Jr. NASA CR-152879, 1977.

45. Kiselev, A.V.; Lygin, V.I. "Infrared Spectra of Surface Compounds"; Halsted Press: New York, 1967; p. 103.

46. Peri, J.B. J. Phys. Chem. 1966, 70, 2937-45.

47. Hercules, D.M. Anal. Chem. 1978, 50, 734A.

48. Sieghbahm, et al. "ESCA. 'Atomic Molecular Solid State Structure Studied by Means of Electron Spectroscopy';" Almquist and Wiksells: Uppsala, 1967.

49. Discuss. Faraday Soc. 60, 1975.

50. Hercules, D.M. Anal. Chem. 1970, 42, 20A.

51. Powell, C.J. Am. Lab., April, 1978.

52. Fadley, C.S. J. Electron Spectrosc. Relat. Phenom. 1974, 5, 725-54.

53. Nefedov, V.I.; Salyn, Ya.V. J. Electron Spectrosc. Relat. Phenom., 1977, 10, 121-4.

54. Tschapek, M.; De Bussetti, S.G.; Ardizzi, G.P. Electro-Anal. Chem. Interfac. Electrochem., 1974, 52, 304-9.

55. Skiles, J.A. MS Theses, Virginia Polytechnic Institute and State University, Blacksburg, Virginia, 1978.

56. Iler, R.K. "The Colloid Chemistry of Silica and Silicates;" Cornell University Press: Ithaca, 1955; p. 259.

57. Kichener, J.A. Discuss. Faraday Soc., 1970-71, 50-52, 379.

58. Nagelschmidt, G.; Gordon, R.L.; Griffin, O.G. Nature, 1952, 169, 539-40.

59. Iler, R.K., private communication, 1978.

60. Scofield, J.H. J. Electron Spectrosc. and Relat. Phenom., 1976, 8, 129-37.

61. Selected Powder Diffraction Data for Minerals, Vol. 2.

62. Edmonds, J.W.; Henslee, W.W.; Guerra, R.E. Anal. Chem., 1977 49, 2196-203.

63. Brown, C.E.; Hall, P.G. Trans. Faraday Soc., 1971, 67, 3558.

64. Seals, R.D.; Alexander, R.; Taylor, L.T.; Dillard, J.G. Inorg. Chem. 1973, 12, 2485.

65. Bailey, R.R.; Wightman, J.P. J. Colloid Interface Sci. (in press).

66. Van Der Marcel, H.W.; Beutelspacher, H. "Atlas of IR of Clay Minerals and Their Admixtures;" Elsevier Scientific Publishing Company: Amsterdam, 1976; p. 326.

67. Dillard, J.G.; Seals, R.D.; Wightman, J.P. Submitted to Atmos. Environ.

68. Pellet, G.L. Private communication, 1978.

APPENDIX I

Computer Program for B.E.T. Surface Area Determination

```
5 DIM X(30),Y(30),E1(30),A(30)
10 DIM W(30),P1(30),P2(30)
15 DIM V(30)
20 READ S
25 LET I1=1
30 READ C1,W1,W2,H1,H2,T1,X1,X2,V1,P4,A1,S1
35 LET W4=W1-W2
40 LET V(1)=0.0
45 LET P2(1)=0.0
50 LET T5=(307.2+T1)/2
55 LET V2=(T1/H2)*((V1*(H1-H2)/307.2)-(3.65*H2/T5))
60 LET I=2
65 READ N
70 READ W(I),P1(I),P2(I)
75 IF W(I)-J .0.0 THEN 100
80 LET Z9=1
85 IF W(I)-1=0.0 THEN 110
90 LET Z9=1
95 IF W(1)-1 0.0 THEN 120
100 LET X3=0.0
105 GO TO 125
110 LET X3=X1
115 GO TO 125
120 LET X3=X2
125 LET A(I)=0.001169*(V1+X3)/W4
130 LET B=((0.3593*V2)/(T1*W4))+(1.311/(T5*W4))
135 LET C=(0.3593*V2*A1)/(W4*T1)
140 LET P5=P2(I-1)
145 LET D=P1(I)-P2(I)
150 LET E=P2(I)-P5
155 LET F=P2(I)**2-P5**2
160 LET G=A(I)*D
165 LET H=8*E
170 LET D1=C*F
175 LET D2=G-H-D1
180 LET V(I)=V(I-1)+D2
185 LET X(I)=P2(I)/P4
190 LET Y(I)=X(I)/(V(I)*(1.0-X(I)))
195 IF N-I+1 0.0 THEN 230
200 Z9=1
205 IF N-I+1=0.0 THEN 230
210 Z9=1
215 IF N-I+1 0.0 THEN 220
220 I=I+1
225 GO TO 70
230 LET S2=0.0
235 LET S3=0.0
240 LET S4=0.0
245 LET S5=0.0
```

```
350 FOR I=2 TO N+1
255 LET S2=S2+X(I)
260 LET S3=S3+Y(I)
265 LET S4=S4+X(I)*Y(I)
270 LET S5=S5+X(I)**2
275 NEXT I
280 LET I5=((S3*S5)-(S2*S4))/((N*S5)-(S2**2))
285 LET L=((N*S4)-(S2*S3))/((N*S5)-(S2**2))
290 LET S6=(0.2687*S1)/(L+I5)
295 LET S7=0.0
300 FOR I=2 TO N+1
305 LET E1(I)=Y(I)-(I5+L*X(I))
310 LET S7=S7+E1(I)**2
315 LET S8=SQR(S7/N)
320 NEXT I
325 PRINT "SAMPLE IDENTIFICATION NO.=";C1,TAB(30);"W1=";W1
326 PRINT "H1=";H1,TAB(15);"X1=";X1,TAB(30);"W1=";W1
327 PRINT "W2=",W2,TAB(15);"H2=";H2,TAB(30);"PS=";P4
328 PRINT "ALPHA=";A1,TAB(15);"WS=";W4,TAB(30);"TS=";T1
329 PRINT "V0=";V1,TAB(15);"S=";S1,TAB(30);"B=";B
330 PRINT "C=";C,TAB(15);"VS=";V2
331 PRINT
332 PRINT
333 PRINT "WHICH X",TAB(20);"X",TAB(40);"Y"
334 FOR I=2 TO N+1
335 LET J=I+1
340 PRINT W(I),TAB(15),X(I),TAB(30),Y(I)
343 PRINT
344 PRINT
345 NEXT I
350 PRINT "SW=";S6
351 PRINT "STANDARD ERROR OF LEAST SQ. LINE =";S8
355 IF S-I1 0.0 THEN 9998
360 L9=1
365 IF S-I1=0.0 THEN 9998
370 LET L9=1
375 IF S-I1>0.0 THEN 380
380 LET I1=I1+1
385 GO TO 30
1005 DATA 1,91.12,58.45
1006 DATA 1,95.55,68.04
1007 DATA 1,99.73,76.30
1008 DATA 1,106.12,84.10
1009 DATA 1,111.51,91.29
1010 DATA 1,123.15,99.42
1011 DATA 1,144.97,111.39
1012 DATA 1,157.84,123.65
9998 STOP
9999 END
```

APPENDIX II

Raw Data For the Adsorption Isotherm Measurements

Sample: Min-U-Sil 5 (A)*

OGT: 100°C (2 hours)

ROGT: 30°C (overnight)

1. Sample weight: 2.0017 g

ADS**		RADS***	
P(torr)	N^s(moles·M^{-2}x10^6)	P(torr)	N^s(moles·M^{-2}x10^6)
7.7	1.689	5.5	0.9626
12.9	1.928	13.9	1.127
18.0	2.410	21.3	1.112
20.5	2.665	27.4	1.367
		34.4	1.708

2. Sample weight: 2.006 g

9.2	1.860	6.1	0.8156
15.0	2.251	12.6	1.046
22.2	2.471	18.9	1.186
29.8	2.834	32.9	1.421

3. Sample weight: 2.0004 g

3.4	1.519	4.3	0.5364
8.1	2.024	10.2	0.5925
13.6	2.152	15.5	0.9057
24.0	2.303	24.1	1.296
32.6	2.650	31.1	1.505

*A: Min-U-Sil batch dated June, 1971.
B: Min-U-Sil batch dated March, 1972.
**ADS: Adsorption
***RADS: Readsorption

Sample: Min-U-Sil 5 (A)

OGT: 200°C (2 hours)

ROGT: 30°C (overnight)

1. Sample weight: 2.0002 g

ADS		RADS	
P(torr)	N^s(moles·M^{-2}x10^6)	P(torr)	N^s(moles·M^{-2}x10^6)
3.9	1.555	4.7	0.5386
10.4	1.816	10.9	0.6079
18.1	1.927	20.3	0.7673
26.5	2.222	26.7	1.014
37.4	2.400	32.7	1.182

2. Sample weight: 2.0038 g

0.6	1.316	4.9	0.2826
7.1	1.728	11.6	0.3834
16.6	2.105	17.9	0.6206
23.1	2.307	28.6	0.8588
32.6	2.659	37.4	1.116

3. Sample weight: 2.0040 g

1.5	1.314	5.7	0.5503
8.0	1.762	13.1	0.7392
14.8	2.145	22.5	0.8844
24.7	2.400	29.3	1.182
35.6	2.687		

4. Sample weight: 2.0041 g

0.9	1.381	4.5	0.7558
8.3	1.861	12.8	0.9990
15.9	2.156	20.7	1.165
24.3	2.455	27.2	1.327
33.8	2.972	35.7	1.534

Sample: Min-U-Sil 5 (A)

OGT: 400°C (2 hours)

ROGT: 30°C (overnight)

1. Sample weight: 2.0010 g

ADS		RADS	
P(torr)	N^s(moles·M^{-2}x10^6)	P(torr)	N^s(moles·M^{-2}x10^6)
1.5	1.746	5.7	0.4552
6.6	1.925	13.0	0.6234
14.8	2.111	21.2	0.7036
23.4	2.246	30.4	0.8174
35.5	2.319	41.5	0.9204

2. Sample weight: 2.0000 g

1.4	1.789	5.6	0.5644
7.7	2.044	13.0	0.6673
14.2	2.281	20.6	0.7762
22.9	2.412	26.6	0.8614
31.6	2.584	36.2	1.092

3. Sample weight: 2.0020 g

0.7	1.718	5.2	0.2671
9.3	2.081	12.7	0.3699
16.0	2.285	19.7	0.5281
23.7	2.372	27.3	0.6222
31.8	2.602	36.2	1.172

4. Sample weight: 2.0024 g

0.3	1.553	3.6	0.4192
6.8	1.710	10.7	0.4984
14.4	1.940	18.5	0.6071
24.2	2.103	26.5	0.7358
31.9	2.283	34.2	0.8297

Sample: Min-U-Sil 5 (A)

OGT: 100°C (2 hours)

ROGT: 100°C (2 hours)

1. Sample weight: 2.0049 g

ADS		RADS	
P(torr)	N^s(moles·M^{-2}x10^6)	P(torr)	N^s(moles·M^{-2}x10^6)
0.7	1.174	1.5	1.312
6.9	1.962	7.5	1.533
13.6	2.491	14.7	1.770
22.8	2.915	21.9	1.921
29.4	3.335	29.5	2.170

2. Sample weight: 2.0027 g

0.9	1.532	1.5	1.253
6.9	2.028	7.0	1.424
11.7	2.313	14.7	1.625
16.6	2.677	22.0	1.812
22.8	3.115	29.3	2.085

Sample: Min-U-Sil 5 (A)

OGT: 100°C (2 hours)

ROGT: 400°C (2 hours)

1. Sample weight: 2.0041 g

1.7	1.682	0.3	1.744
7.3	2.087	5.8	1.988
13.3	2.483	12.8	2.224
18.6	2.806	19.4	2.406
24.3	3.119	26.6	2.562

Sample: Iler treated Min-U-Sil (B)

OGT: 100°C (2 hours)

ROGT: 30°C (overnight)

1. Sample weight: 2.0035 g

ADS		RADS	
P(torr)	N^s(moles·M^{-2}x10^6)	P(torr)	N^s(moles·M^{-2}x10^6)
2.2	1.604	5.5	0.4686
9.9	1.879	12.6	0.5962
18.4	2.129	21.9	0.7522
25.1	2.493	29.5	1.041
31.9	2.772	37.1	1.229

2. Sample weight: 2.0026 g

2.7	1.651	4.7	0.4584
9.7	1.981	12.2	0.5717
17.3	2.265	18.7	0.7498
25.9	2.597	27.1	0.8543
33.7	2.968	34.8	1.019

Sample: Min-U-Sil 5 (B)

OGT: 400°C (2 hours)

ROGT: 400°C (2 hours)

1. Sample weight: 2.0002 g

ADS		RADS	
P(torr)	N^s(moles·M^{-2}x10^6)	P(torr)	N^s(moles·M^{-2}x10^6)
0.9	1.466	0.1	1.358
8.7	1.689	6.5	1.690
16.3	1.907	13.6	1.839
24.2	2.038	19.9	1.988
33.5	2.103	27.9	2.089

2. Sample weight: 2.0036 g

2.7	1.474	0.9	1.613
9.8	1.628	8.7	1.777
16.5	1.748	15.6	1.947
25.1	1.872	23.6	2.053
32.9	1.994	30.4	2.273

3. Sample weight: 2.0000 g

1.1	1.478	1.3	1.636
9.9	1.661	10.6	1.822
16.9	1.843	17.5	1.946
26.1	1.931	25.0	2.069
34.0	2.026	33.2	2.101

Sample: Min-U-Sil 5 (A)

OGT: 400°C (2 hours)

ROGT: 100°C (2 hours)

1. Sample weight: 2.0006 g

ADS		RADS	
P(torr)	N^s(moles·M^{-2}x10^6)	P(torr)	N^s(moles·M^{-2}x10^6)
0.9	1.511	4.5	0.7325
7.9	2.154	11.5	0.8523
15.0	2.287	20.2	0.9741
22.8	2.434	26.4	1.047
29.6	2.634	32.8	1.191

Sample: Min-U-Sil 5 (B)

OGT: 100°C (2 hours)

1. Sample weight: 2.0033 g

3.5	1.245
10.9	1.530
18.9	1.856
26.7	2.137

2. Sample weight: 2.0059 g

1.1	1.072
5.6	1.404
12.1	1.606
18.1	1.872
24.8	2.141

Sample: NASA #2

OGT: 100°C (2 hours)

Weight: 2.0049 g

P(torr)	N^s(moles·M^{-2}x10^5)
2.1	1.323
7.4	1.670
13.7	2.092
19.4	2.367
28.0	2.697

Sample: NASA #4

OGT: 100°C (2 hours)

Weight: 2.0080 g

P(torr)	N^s(moles·M^{-2}x10^5)
2.7	3.670
8.6	4.862
15.1	5.702
22.0	6.592
30.1	7.882

Sample: Empty sample bulb

OGT: 100°C (2 hours)

P(torr)	N^s(moles x 10^6)
7.3	--
15.4	0.02309
22.4	0.5980
29.0	1.211
35.6	1.434

P(torr)	N^s(moles x 10^6)
6.8	0.0072
15.1	0.0045
23.4	1.228
31.2	2.208
38.4	3.938